Compton Sources of Electromagnetic Radiation*

Geoffrey A. Krafft
Jefferson Lab, Old Dominion University
Gerd Priebe
Max Born Institute

*Reviews of Accelerator Science and Technology, **3**, 147 (2010)

Outline

- Basic Physics
  - Compton Effect
  - Energy
  - Flux
  - Energy Spread
  - Pulse Length
  - Brilliance
  - Harmonics/ Broadening
- Laser Performance
  - Self-Excited Arrangements
  - External High Power Optical Cavities
  - High Peak Power

- Ring Sources
  - Direct Illumination
  - Self Excited
  - External Cavities
- Linac/ERL Based Sources
  - Self Excited
  - Direct Illumination
- Future Proposals
  - X-Rays
  - Gamma-Rays
- Conclusions

Compton Effect

TABLE I

Wave-length of Primary and Scattered γ-rays

	Angle	μ/ρ	τ/ρ	λ obs.	λ calc.
Primary..........	0°	.076	.017	0.022 A	(0.022 A)
Scattered.........	45°	.10	.042	.030	0.029
"	90°	.21	.123	.043	0.047
"	135°	.59	.502	.068	0.063

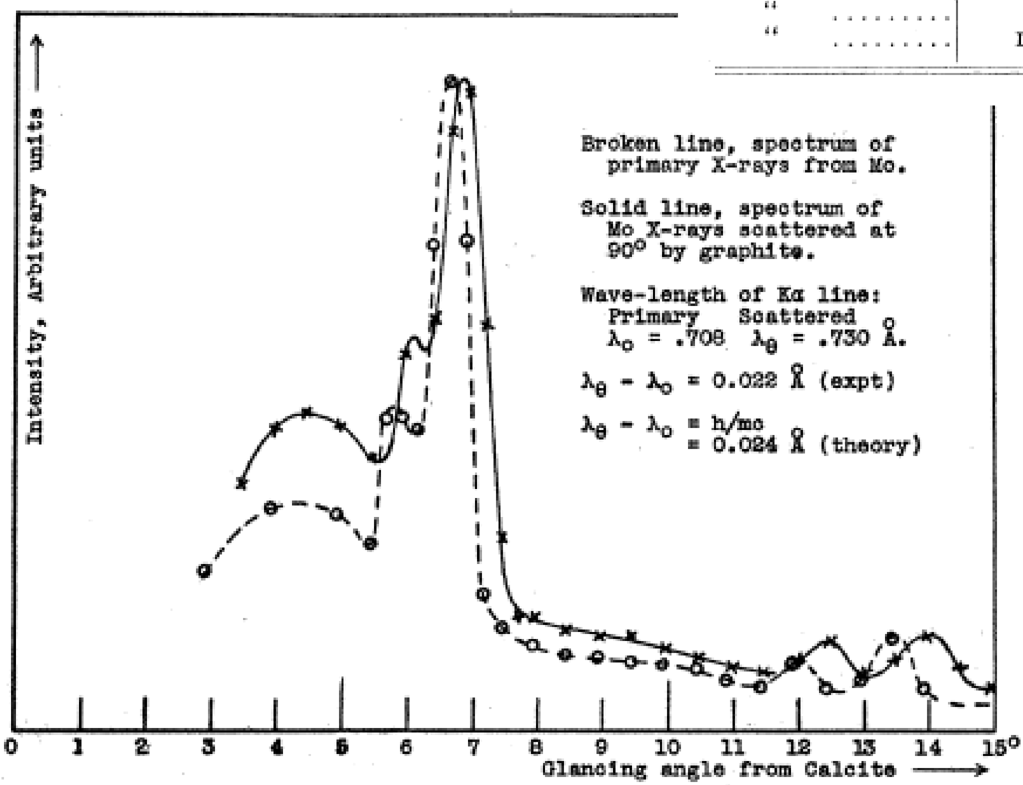

Fig. 4. Spectrum of molybdenum X-rays scattered by graphite, compared with the spectrum of the primary X-rays, showing an increase in wave-length on scattering.

A. H. Compton, Phys. Rev., 21, 483 (1923)

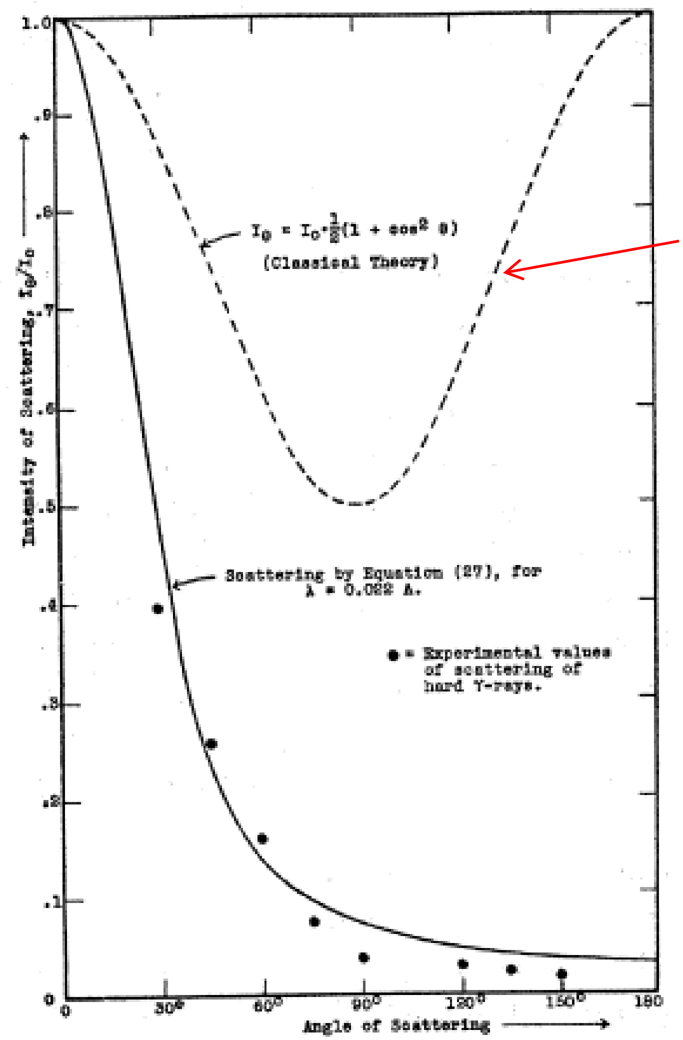

Unpolarized Incident X-ray Beam

Fig. 7. Comparison of experimental and theoretical intensities of scattered γ-rays.

Energy

- Layout

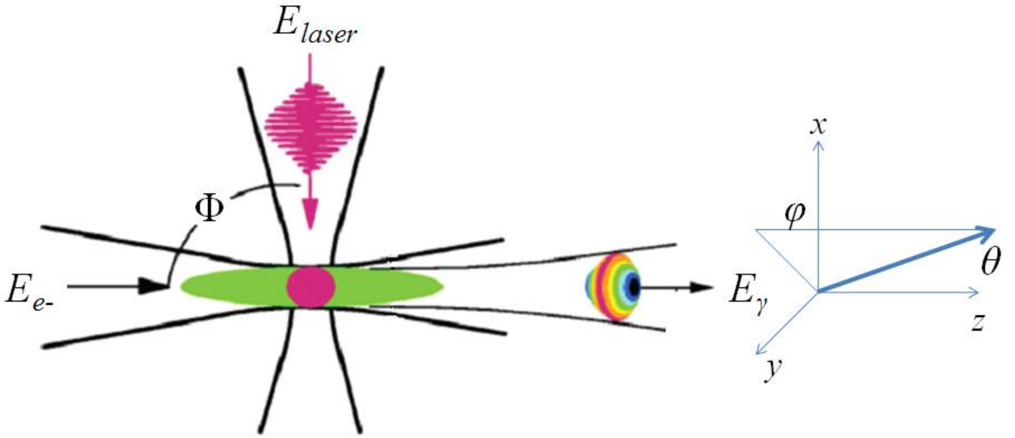

- Energy

$$E_\gamma(\theta,\varphi) = \frac{E_{\text{laser}}(1-\beta\cos\Phi)}{1-\beta\cos\theta + E_{\text{laser}}(1-\cos\Delta\Theta)/E_{e^-}}$$

- Thomson limit

$$E'_{\text{laser}} << mc^2, \qquad E_\gamma\ \ \theta,\phi\ \approx E_{\text{laser}}\frac{1-\beta\cos\Phi}{1-\beta\cos\theta}$$

Field Strength Parameter

- Early 1960s: Laser Invented
- Brown and Kibble (1964): Earliest definition of the field strength parameters (normalized vector potential) *K* and/or *a* in the literature that I'm aware of

  $$a = \frac{eE_0\lambda_0}{2\pi mc^2} \quad \text{Compton/Thomson Sources} \qquad K = \frac{eB_0\lambda_0}{2\pi mc} \quad \text{Undulators}$$

  Interpreted frequency shifts that occur at high fields as a "relativistic mass shift".
- Sarachik and Schappert (1970): Power into harmonics at high *K* and/or *a* . Full calculation for CW (monochromatic) laser. Later referenced, corrected, and extended by workers in fusion plasma diagnostics.
- Alferov, Bashmakov, and Bessonov (1974): Undulator/Insertion Device theories developed under the assumption of constant field strength. Numerical codes developed to calculate "real" fields in undulaters.
- Coisson (1979): Simplified undulater theory, which works at low *K* and/or *a,* developed to understand the frequency distribution of "edge" emission, or emission from "short" magnets, i.e., including pulse effects

Spectrum from a "Short" Magnet

Coisson low-field strength undulater spectrum*

$$\frac{dU_\gamma}{d\nu d\Omega} = \frac{r_e^2 c}{\pi} \gamma^2 \left(1+\gamma^2\theta^2\right)^2 f^2 \left|\tilde{B}\left(\nu\left(1+\gamma^2\theta^2\right)/2\gamma^2\right)\right|^2$$

$$f^2 = f_\sigma^2 + f_\pi^2$$

$$f_\sigma = \frac{1}{\left(1+\gamma^2\theta^2\right)^2}\sin\phi$$

$$f_\pi = \frac{1}{\left(1+\gamma^2\theta^2\right)^2}\left(\frac{1-\gamma^2\theta^2}{1+\gamma^2\theta^2}\right)\cos\phi$$

$$r_e^2 \equiv \frac{e^4}{16\pi^2\varepsilon_0^2 m^2 c^4}$$

*R. Coisson, Phys. Rev. A **20**, 524 (1979)

Dipole Radiation

$$\vec{B} = \frac{\mu_0 e\ddot{d}\ \ t - r/c}{4\pi c r}\sin\Theta\hat{\Phi}$$

$$\vec{E} = \frac{\mu_0 e\ddot{d}\ \ t - r/c}{4\pi r}\sin\Theta\hat{\Theta}$$

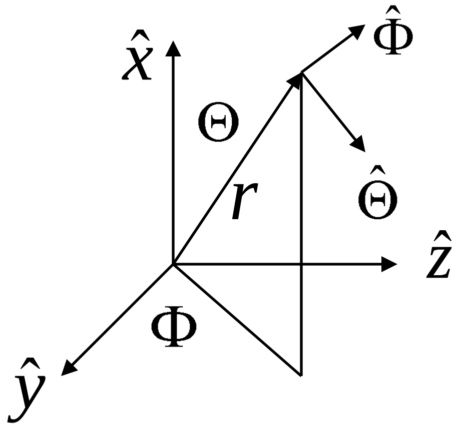

$$I = \frac{\vec{E}\times\vec{B}}{\mu_0} = \frac{\mu_0}{16\pi^2}\frac{e^2\ddot{d}^2\ \ t - r/c}{c r^2}\sin^2\Theta\hat{r}$$

$$\frac{dI}{d\Omega} = \frac{1}{16\pi^2\varepsilon_0}\frac{e^2\ddot{d}^2\ \ t - r/c}{c^3}\sin^2\Theta$$

Polarized in the plane containing $\hat{r} = \vec{n}$ and $\hat{x}$

Dipole Radiation

Define the Fourier Transform

$$\tilde{d}(\omega) = \int d(t) e^{-i\omega t} dt \qquad\qquad d(t) = \frac{1}{2\pi}\int \tilde{d}(\omega) e^{i\omega t} d\omega$$

With these conventions Parseval's Theorem is

$$\int d^2(t)\, dt = \frac{1}{2\pi}\int \left|\tilde{d}\right|^2 (\omega)\, d\omega$$

$$\frac{dU_\gamma}{d\Omega} = \frac{e^2}{16\pi^2\varepsilon_0 c^3}\int \ddot{d}^2\left(t - r/c\right) dt = \frac{e^2}{32\pi^3\varepsilon_0 c^3}\int \omega^4 \left|\tilde{d}\right|^2 (\omega)\, d\omega$$

$$\frac{dU_\gamma}{d\omega d\Omega} = \frac{1}{32\pi^3\varepsilon_0}\frac{e^2\omega^4\left|\tilde{d}(\omega)\right|^2}{c^3}\sin^2(\Theta)$$

Blue Sky!

This equation does not follow the typical (see Jackson) convention that combines both positive and negative frequencies together in a single positive frequency integral. The reason is that we would like to apply Parseval's Theorem easily. By symmetry, the difference is a factor of two.

Comments/Sum Rule

- There is no radiation parallel or anti-parallel to the *x*-axis for *x*-dipole motion (gives the 0.5 in Compton's curve)
- In the forward direction $\theta' \rightarrow 0$, the radiation polarization is parallel to the *x*-axis for an *x*-dipole motion

$$\frac{dU'_{\gamma,\sigma}}{d\omega'} = \frac{1}{32\pi^3\varepsilon_0}\frac{e^2\omega'^4}{c^3}\left|\tilde{d}'_x\;\;\omega'\right|^2 + \left|\tilde{d}'_y\;\;\omega'\right|^2\;\;2\pi$$

$$\frac{dU'_{\gamma,\pi}}{d\omega'} = \frac{1}{32\pi^3\varepsilon_0}\frac{e^2\omega'^4}{c^3}\left[\;\left|\tilde{d}'_x\;\;\omega'\right|^2 + \left|\tilde{d}'_y\;\;\omega'\right|^2\frac{2\pi}{3} + \left|\tilde{d}'_z\;\;\omega'\right|^2\frac{8\pi}{3}\right]$$

$$\frac{dU'_{\gamma}}{d\omega'} = \frac{1}{32\pi^3\varepsilon_0}\frac{e^2\omega'^4\left|\tilde{\vec{d}}'\;\;\omega'\right|^2}{c^3}\frac{8\pi}{3}$$

Generalized Larmor (in frequency space)

Sum Rule

Total energy sum rule

$$U_{tot}^{'} = \int_{-\infty}^{\infty} \frac{1}{12\pi^2\varepsilon_0} \frac{e^2\omega'^4 \left|\tilde{\vec{d}}' \quad \omega'\right|^2}{c^3} d\omega'$$

Parseval’s Theorem again gives “standard” Larmor formula

$$P' = \frac{dU_{tot}^{'}}{dt'} = \frac{1}{6\pi\varepsilon_0} \frac{e^2 \ddot{\vec{d}}'^2 \quad t'}{c^3} = \frac{1}{6\pi\varepsilon_0} \frac{e^2 \vec{a}'^2 \quad t'}{c^3}$$

Weak Field Undulator Spectrum

$$\tilde{\vec{d}}'(\omega') = \tilde{d}'(\omega')\hat{x} = -\frac{ec}{mc^2}\frac{\tilde{B}(\omega'/c\beta_z\gamma)}{\omega'^2}\hat{x} \qquad \tilde{B}(k) = \int B(z)e^{-ikz}dz$$

$$\frac{dU_{\gamma,\sigma}}{d\omega d\Omega} = \frac{1}{32\pi^3\varepsilon_0}\frac{e^4}{m^2c^5}\frac{\left|\tilde{B}\left(\omega\left(1-\beta_z\cos\theta\right)/c\beta_z\right)\right|^2}{\gamma^2\left(1-\beta_z\cos\theta\right)^2}\sin^2\phi$$

$$\frac{dU_{\gamma,\pi}}{d\omega d\Omega} = \frac{1}{32\pi^3\varepsilon_0}\frac{e^4}{m^2c^5}\frac{\left|\tilde{B}\left(\omega\left(1-\beta_z\cos\theta\right)/c\beta_z\right)\right|^2}{\gamma^2\left(1-\beta_z\cos\theta\right)^2}\left(\frac{\cos\theta-\beta_z}{1-\beta_z\cos\theta}\right)^2\cos^2\phi$$

$$\lambda = \frac{\lambda_0}{2\gamma^2} \qquad \left(1-\beta_z\cos\theta\right)\left(1+\beta_z\right) \approx \frac{1}{\gamma^2}+\theta^2+\ldots \approx \frac{1+\gamma^2\theta^2}{\gamma^2}$$

Generalizes Coisson to arbitrary observation angles

Weak Field Thomson Backscatter

With Φ = *π* and *a* << 1 the result is identical to the weak field undulator result with the replacement of the magnetic field Fourier transform by the electric field Fourier transform

	Undulator	Thomson Backscatter
Driving Field	$\tilde{B}_y\left(\omega(1-\beta_z\cos\theta)/c\beta_z\right)$	$\tilde{E}_x\left(\omega(1-\beta_z\cos\theta)/(c(1+\beta_z))\right)$
Forward Frequency	$\lambda \approx \frac{\lambda_0}{2\gamma^2}$	$\lambda \approx \frac{\lambda_0}{4\gamma^2}$
	Lorentz contract + Doppler	Double Doppler

Handy Formulas

$$\frac{d^2U_\gamma}{d\omega d\Omega} = \frac{r_e^2\varepsilon_0}{2\pi c}\left|\tilde{E}\left[\frac{\omega\ \ 1-\beta\cos\theta}{c\ \ 1+\beta}\right]\right|^2 \times$$

$$\frac{\sin^2\phi\ \ 1-\beta\cos\theta\ \ ^2 + \cos^2\phi\ \ \cos\theta-\beta\ \ ^2}{\gamma^2\ \ 1-\beta\cos\theta\ \ ^{2\cdot 2}}$$

$$U_\gamma = \gamma^2\ \ 1+\beta\ \ \frac{N_e\sigma_T}{\sigma_e^2+\sigma_{laser}^2}$$

$$N_\gamma = \sigma_T\frac{N_e N_{laser}}{2\pi\ \ \sigma_e^2+\sigma_{laser}^2}$$

$$N_{\gamma,\text{per } e} = \frac{2\pi\alpha N_\lambda a^2}{3}$$

Number Distribution of Photons

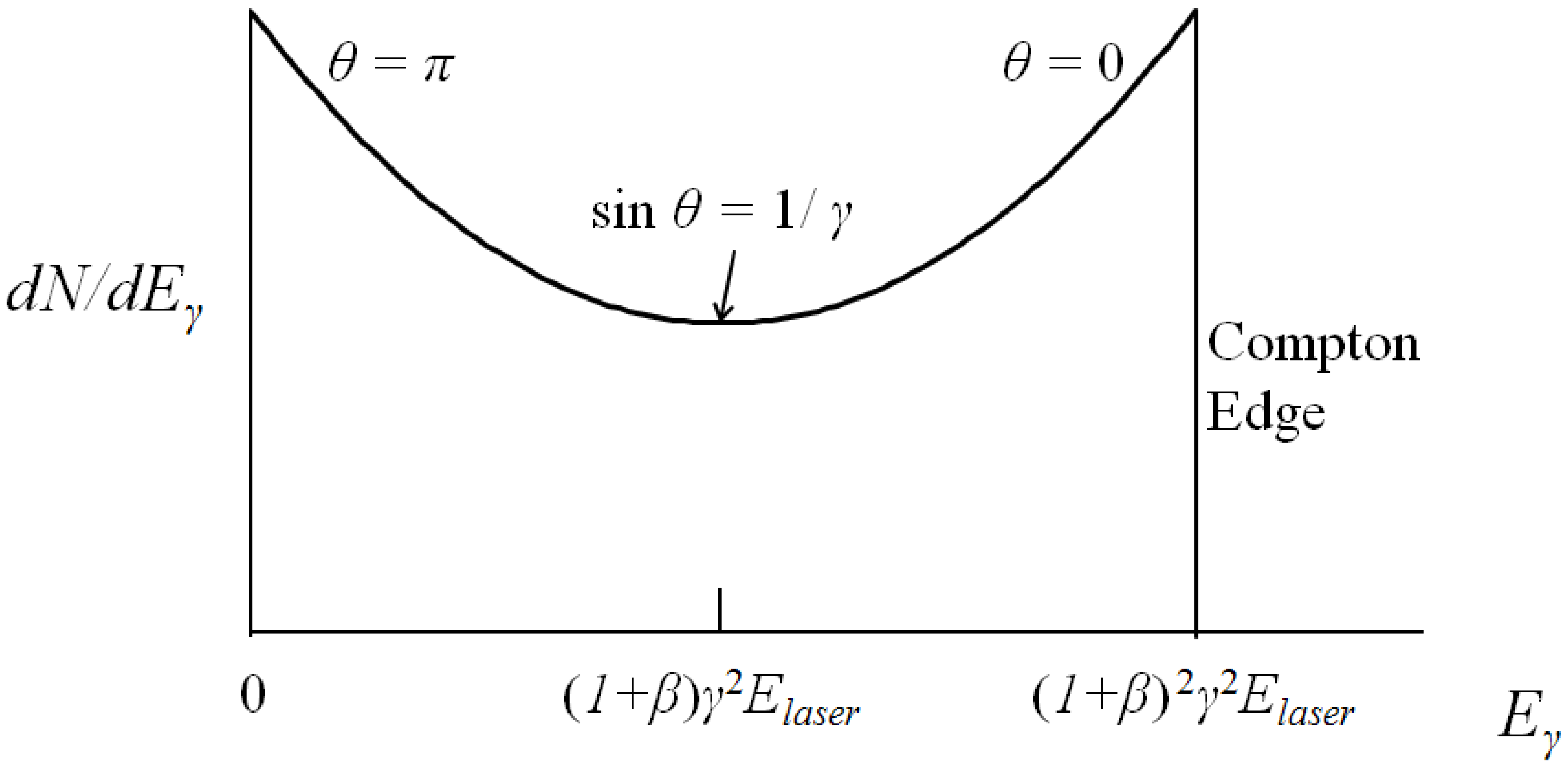

Flux

- Percentage in 0.1% bandwidth ($\theta = 0$)

$$N_{0.1\%} = 1.5 \times 10^{-3} N_\gamma$$

- Flux into 0.1% bandwidth

$$\mathcal{F} = 1.5 \times 10^{-3} \dot{N}_\gamma$$

- Flux for high rep rate source

$$\mathcal{F} = 1.5 \times 10^{-3} f N_\gamma$$

Energy Spread

Sources of Energy Spread in the Scattered Pulse

Source Term	Estimate	Comment
Beam energy spread	$2\sigma_{E_{e-}} / E_{e-}$	From FEL resonance
Laser pulse width	σ_{ω} / ω	Doppler Freq Indepedent
Finite θ acceptance (full width)	$\gamma^2 \Delta\theta^2$	$\theta = 0$ for experiments
Finite beam emittance	$2\gamma^2 \varepsilon / \beta_{e-}$	Beta-function

Spectral Brilliance

- In general

$$\mathcal{B} = \frac{\mathcal{F}}{4\pi^2 \sigma_x \sigma_{x'} \sigma_y \sigma_{y'}}$$

$$\approx \frac{\mathcal{F}}{4\pi^2 \sqrt{\beta_x \varepsilon_x} \sqrt{\varepsilon_x / \beta_x + \lambda / 2L} \sqrt{\beta_y \varepsilon_y} \sqrt{\varepsilon_y / \beta_y + \lambda / 2L}}$$

- For Compton scattering from a low energy beam

$$\mathcal{B} = \frac{\mathcal{F}}{4\pi^2 \varepsilon_x \varepsilon_y}$$

Compton Polarimetry

- At high photon energy (in beam frame), scattering rate couples to the polarization variables

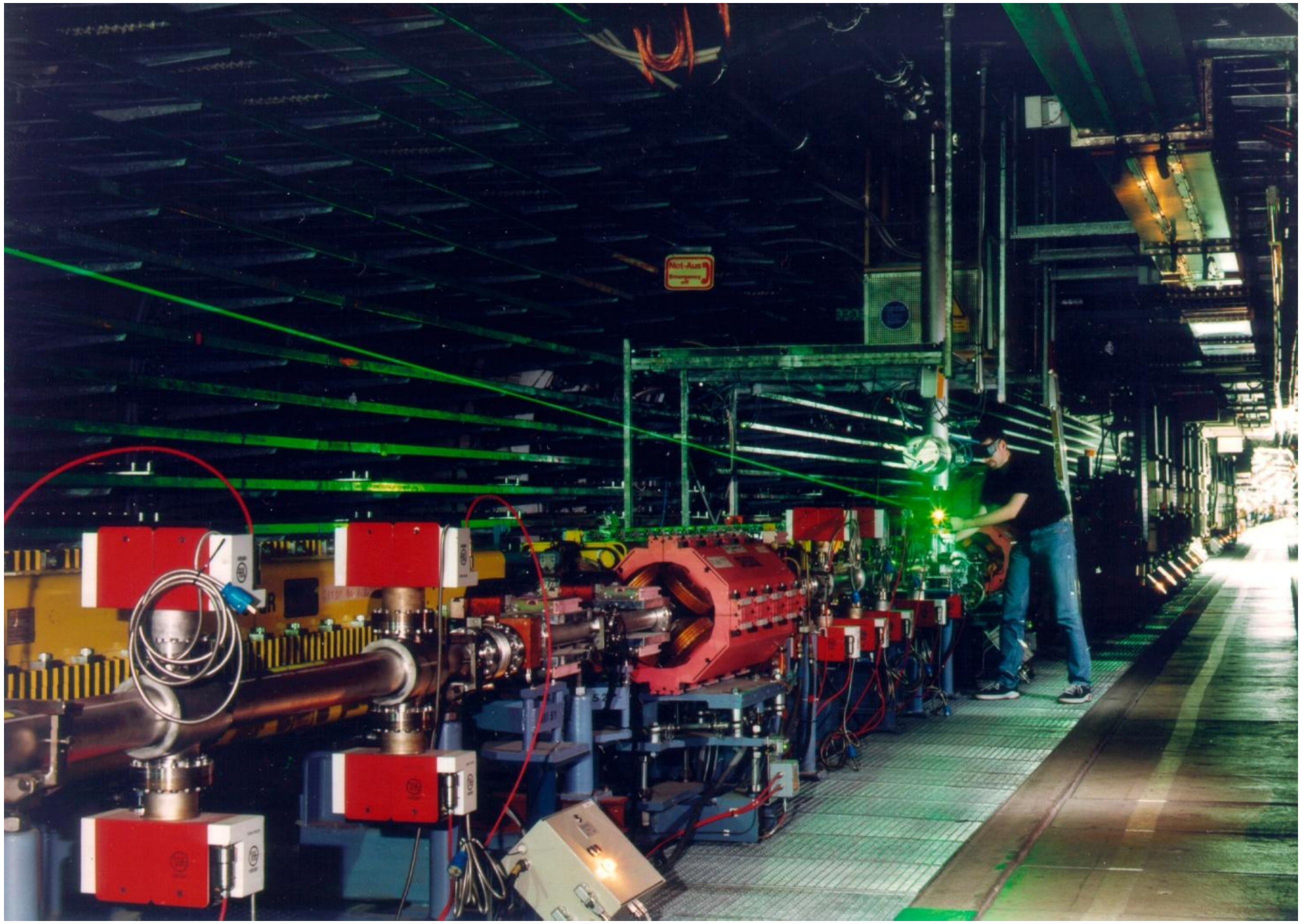

High a/K

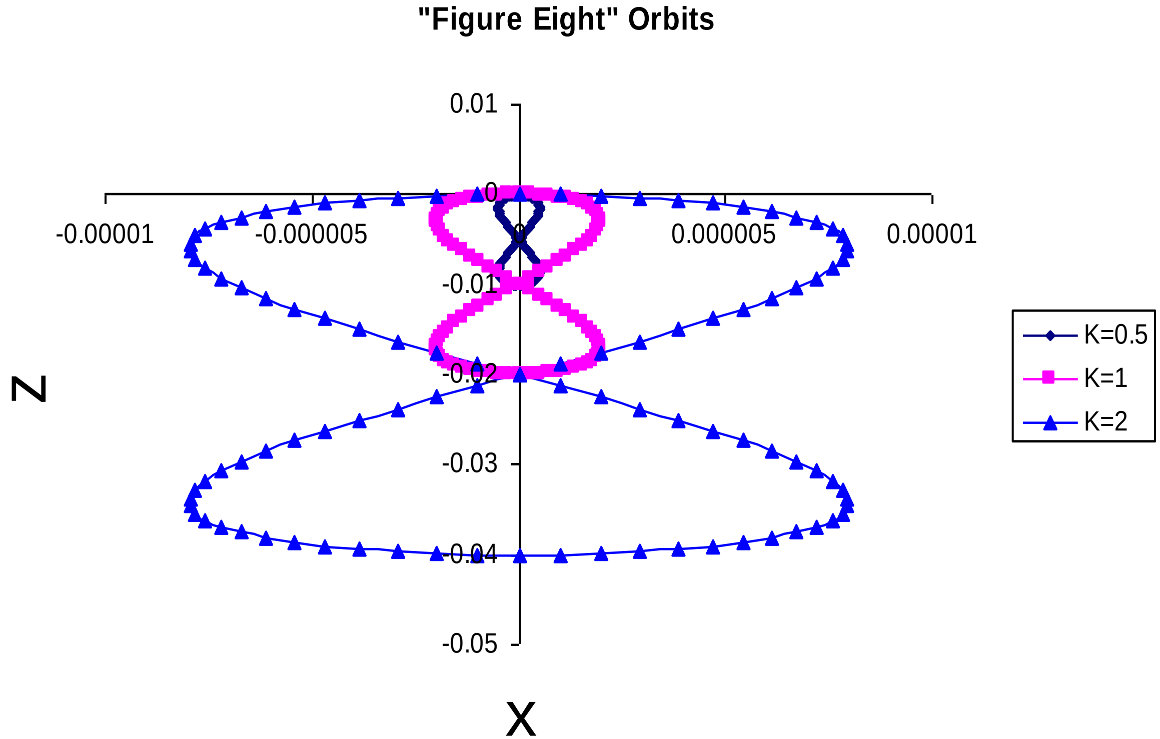

γ = 100, distances are normalized by $\lambda_0 / 2\pi$

Energy Distribution

$$\frac{dU_{\gamma,\sigma}}{d\omega d\Omega} = \frac{e^2\omega^2}{32\pi^3\varepsilon_0 c^3}\left| \begin{array}{c} D_t(\omega;\theta,\varphi)\sin\varphi \\ -\dfrac{\sin\Phi}{\gamma(1-\beta\cos\Phi)} D_p(\omega;\theta,\varphi)\cos\varphi \end{array} \right|^2$$

$$\frac{dU_{\gamma,\pi}}{d\omega d\Omega} = \frac{e^2\omega^2}{32\pi^3\varepsilon_0 c^3}\left| \begin{array}{c} D_t(\omega;\theta,\varphi)\left(\dfrac{\cos\theta-\beta}{1-\beta\cos\theta}\right)\cos\varphi \\ +\dfrac{\sin\Phi}{\gamma(1-\beta\cos\Phi)} D_p(\omega;\theta,\varphi)\left(\dfrac{\cos\theta-\beta}{1-\beta\cos\theta}\right)\sin\varphi \\ +\left(\dfrac{\beta-\cos\Phi}{1-\beta\cos\Phi}\right) D_p(\omega;\theta,\varphi)\left(\dfrac{\sin\theta}{\gamma(1-\beta\cos\theta)}\right) \end{array} \right|^2$$

Effective Dipole Motions

$$D_t(\omega;\theta,\varphi)=\frac{1}{\gamma(1-\beta\cos\Phi)}\int\frac{eA(\xi)}{mc}e^{i\phi(\omega,\xi;\theta,\varphi)}d\xi$$

$$D_p(\omega;\theta,\varphi)=\frac{1}{\gamma(1-\beta\cos\Phi)}\int\frac{e^2A^2(\xi)}{2m^2c^2}e^{i\phi(\omega,\xi;\theta,\varphi)}d\xi$$

And the (Lorentz invariant!) phase is

$$\varphi(\omega,\xi;\theta,\phi)=\frac{\omega}{c}\left(\xi\frac{1-\beta\cos\theta}{1-\beta\cos\Phi}-\frac{\sin\theta\cos\phi}{\gamma(1-\beta\cos\Phi)}\int_{-\infty}^{\xi}\frac{eA(\xi')}{mc}d\xi'+\frac{1-\sin\theta\sin\phi\sin\Phi-\cos\theta\cos\Phi}{\gamma^2(1-\beta\cos\Phi)^2}\int_{-\infty}^{\xi}\frac{e^2A^2(\xi')}{2m^2c^2}d\xi'\right)$$

High Field Thomson Backscatter

For a flat incident laser pulse the main results are very similar to those from undulaters with the following correspondences

	Undulater	Thomson Backscatter
Field Strength	K	a
Forward Frequency	$\lambda \approx \frac{\lambda_0}{2\gamma^2}\left(1+\frac{K^2}{2}\right)$	$\lambda \approx \frac{\lambda_0}{4\gamma^2}\left(1+\frac{a^2}{2}\right)$
Transverse Pattern	$\beta^*_z + \cos\theta'$	$1+\cos\theta'$

NB, be careful with the radiation pattern, it is the same at small angles, but quite a bit different at large angles

Modifications at High *a*

- Resonance frequency in forward direction red-shifts

$$E_{\gamma,n} = n\frac{4\gamma^2 E_{laser}}{1+a^2/2}$$

- Flux into the *n*th harmonic (*n* odd)

$$F_n(a) = \frac{n^2 a^2}{(1+a^2/2)^2}\left\{ J_{(n-1)/2}\left[\frac{na^2}{4(1+a^2/2)}\right] - J_{(n+1)/2}\left[\frac{na^2}{4(1+a^2/2)}\right] \right\}$$

- Non-flat illumination pulses give ponderomotive broadening

Flat Illumination Pulse

20-period
equivalent undulater: $A_x(\xi) = A_0 \cos(2\pi\xi/\lambda_0)\left[\Theta(\xi) - \Theta(\xi - 20\lambda_0)\right]$

$$\omega_0 \equiv (1+\beta_z)^2 \gamma^2 2\pi c/\lambda_0 \approx 4\gamma^2 2\pi c/\lambda_0, \quad a = eA_0/mc$$

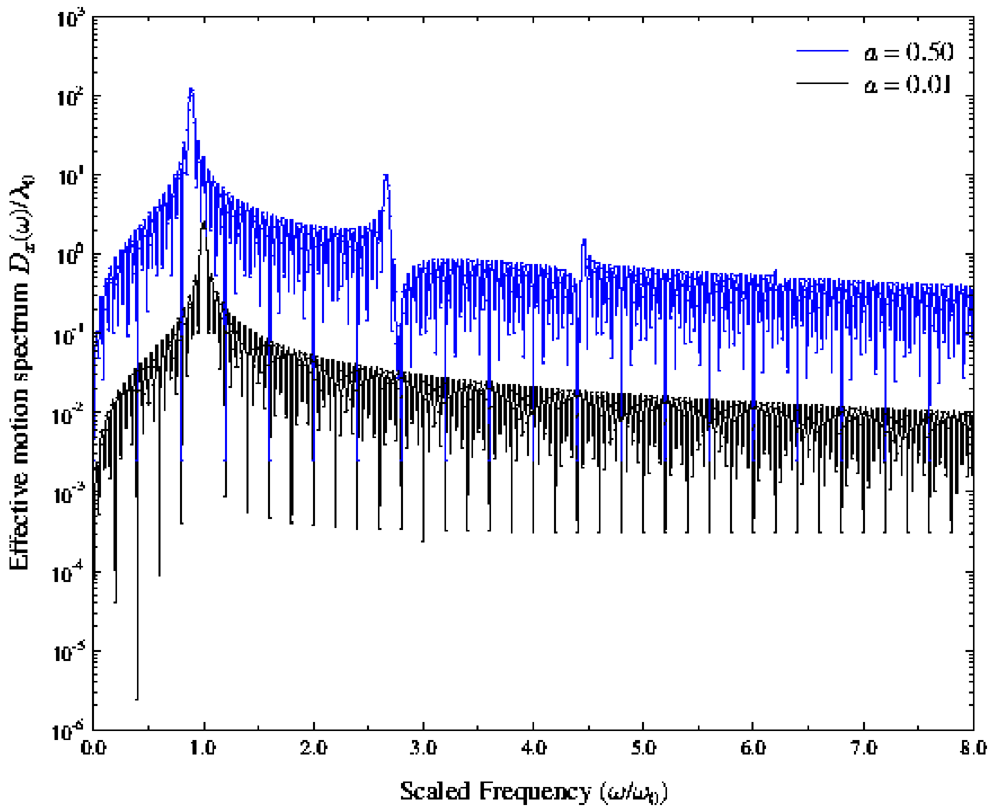

$$1/\left(1+a^2/2\right)$$

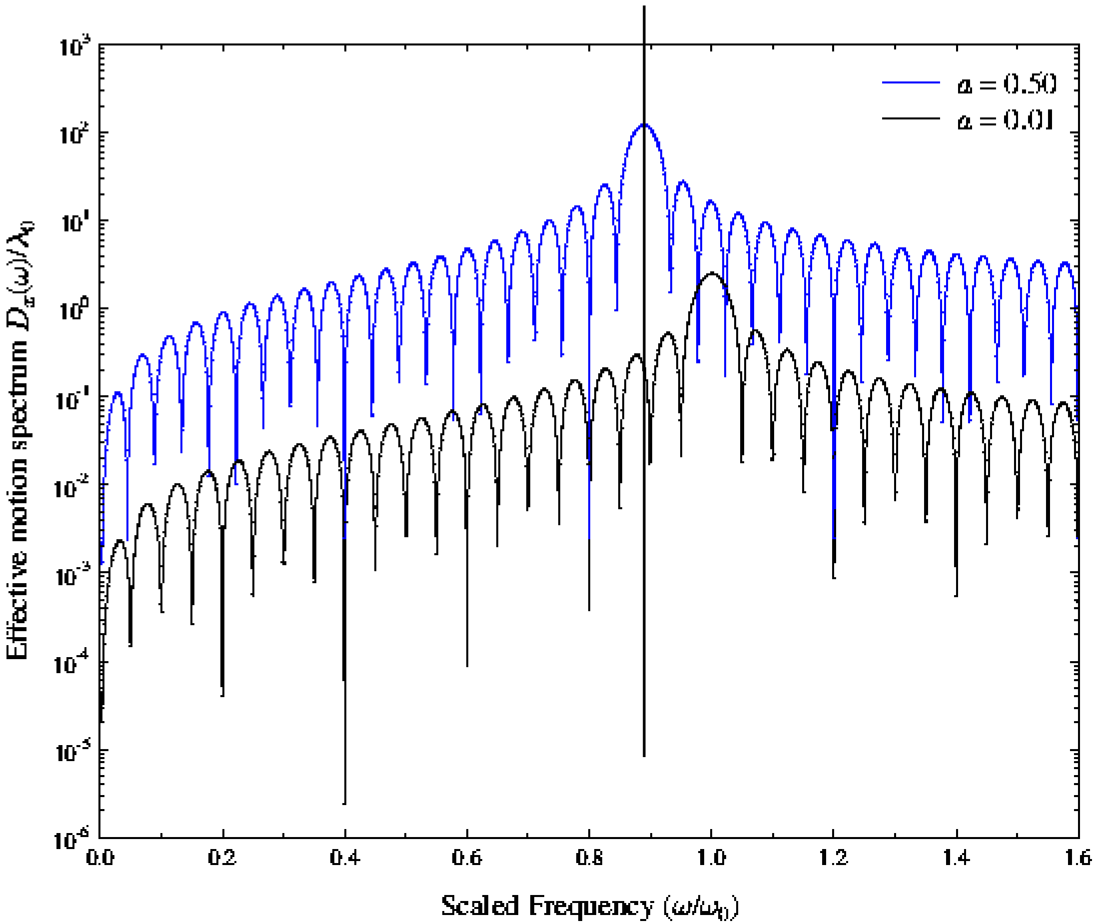

Spectral Broadening: Gaussian Pulse

$$A_x(\xi) = A_{peak}\exp\left(-z^2/2(3.156\lambda_0)^2\right)\cos(2\pi\xi/\lambda_0) \qquad a_{peak} = eA_{peak}/mc$$

A_{peak} and λ_0 chosen for same intensity and same *rms* pulse length as previous slide

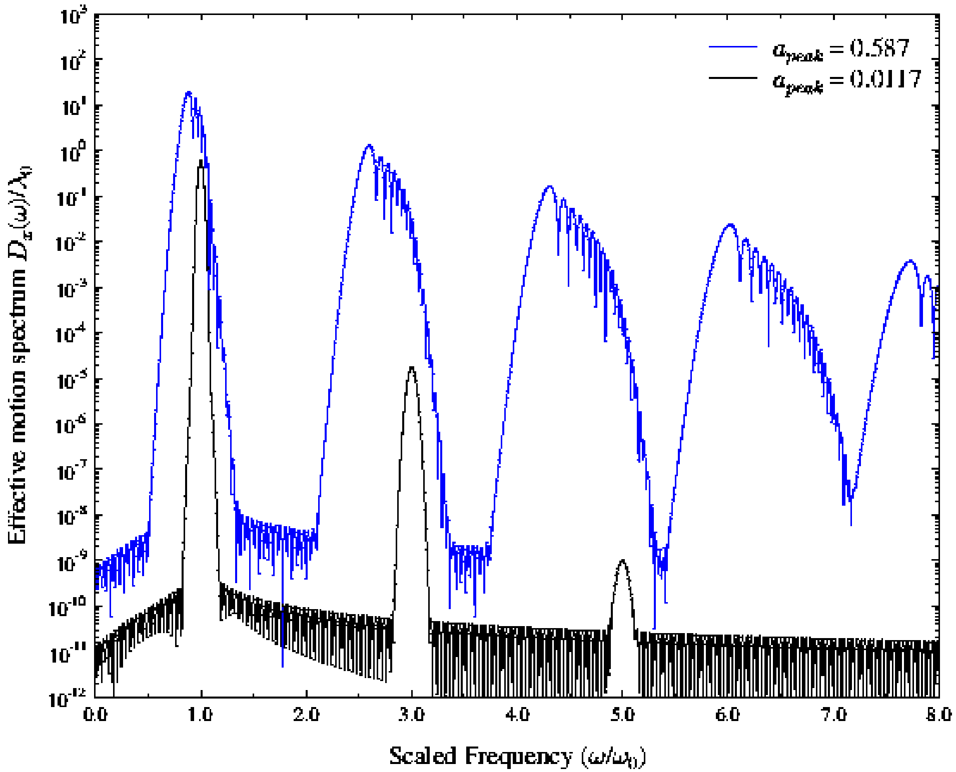

G. A. Krafft, Phys. Rev. Lett., **92**, 204802 (2004)

Source Illumination Method

- Direct illumination by laser
  - Earliest method
  - Deployed on storage rings
- Optical cavities
  - Self-excited
  - Externally excited
  - Deployed on rings, linacs, and energy recovered linacs
- High power single pulses
  - Deployed on linacs

Early Gamma Ray Sources

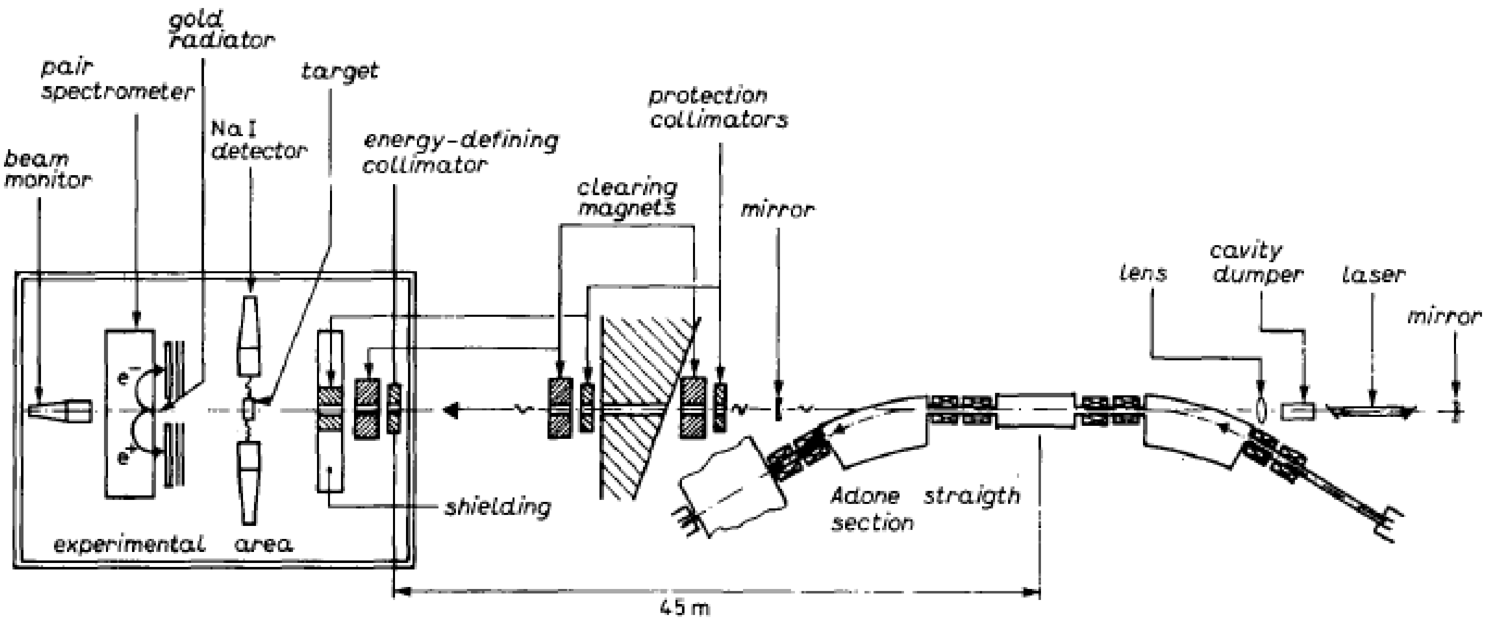

Fig. 1. – Overall view of the experimental set-up.

Compton Edge
78 MeV

Federici, *et al.*
Nouvo. Cim. B 59, 247 (1980)

LEGS

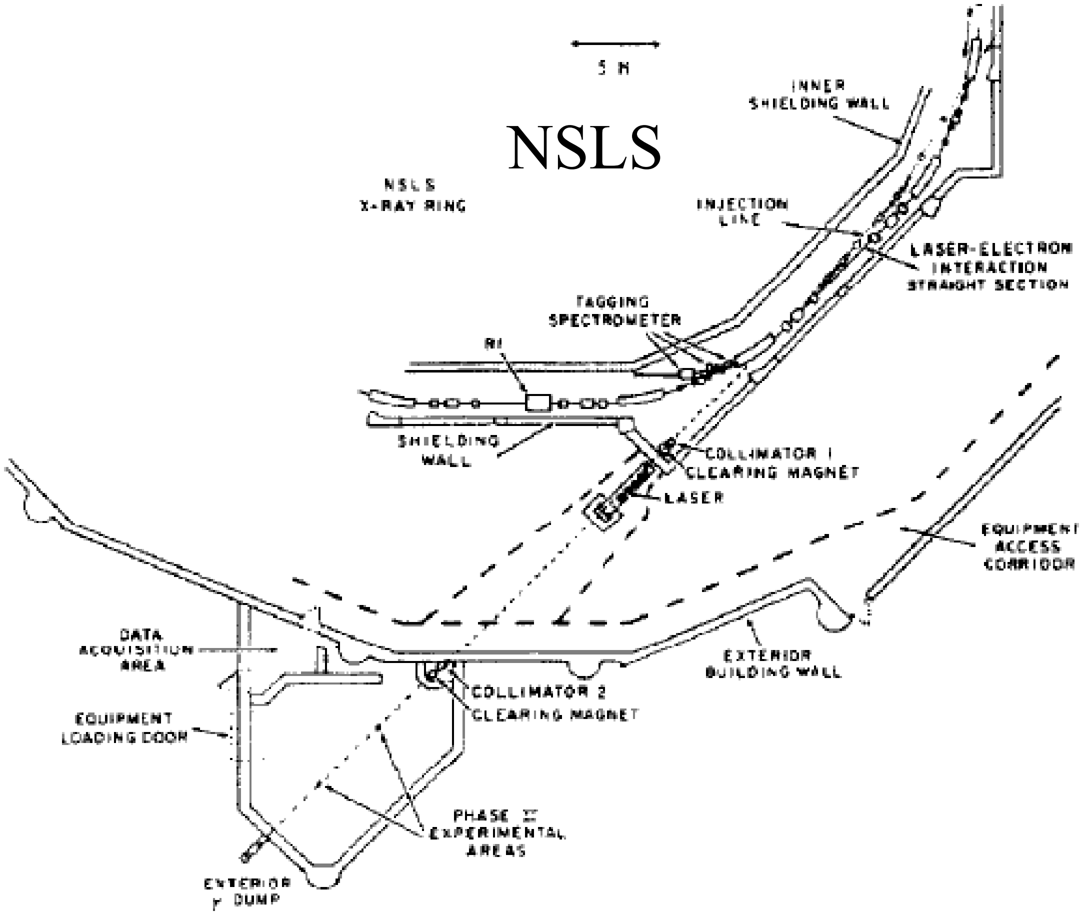

Fig. 4 A plan of the LEGS facility at BNL.

Compton Edge
270 MeV

Sandorfi, *et al.*
PAC83, 3083 (1983)

Electrotechnical Laboratory (Japan)

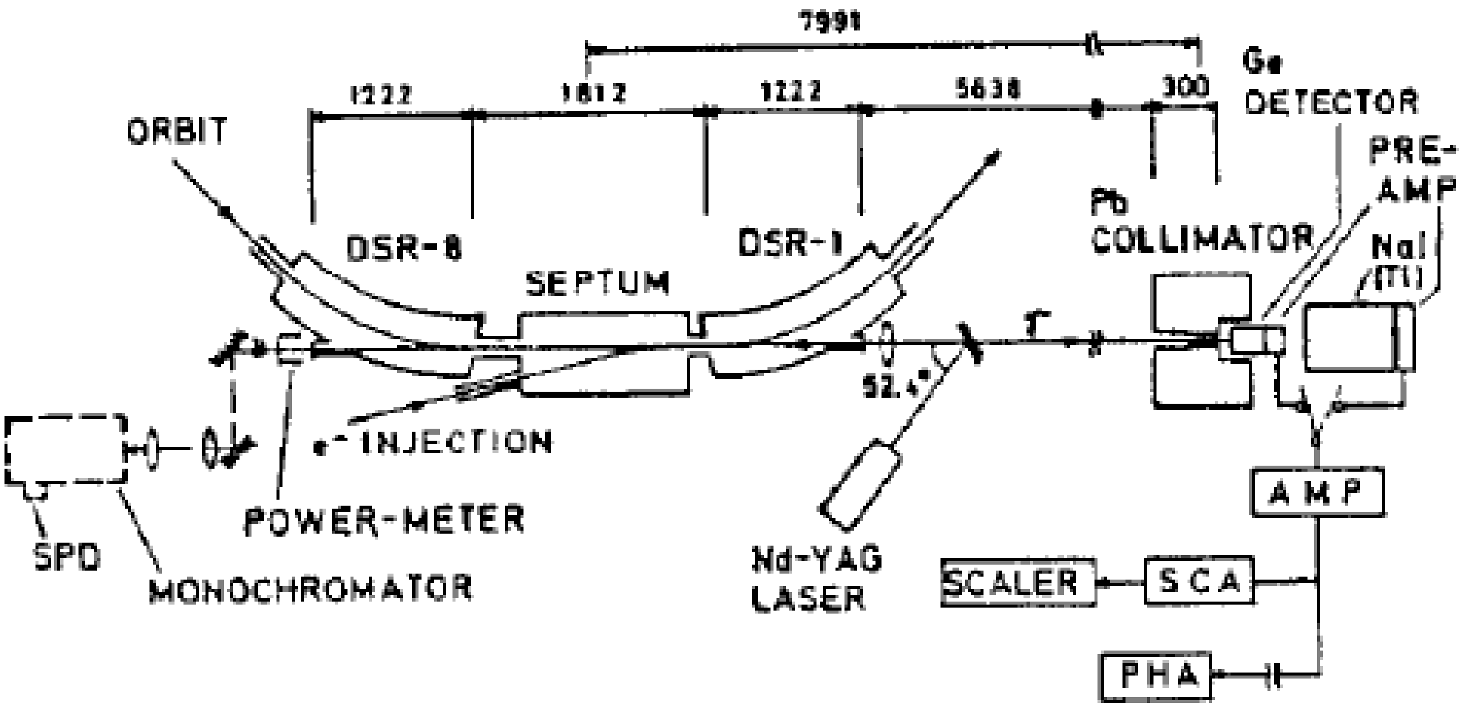

Fig. 2. Experimental arrangement.

Compton Edge 6.5 MeV

Yamazaki, *et al.*
PAC85, 3406 (1985)

Optical Cavities

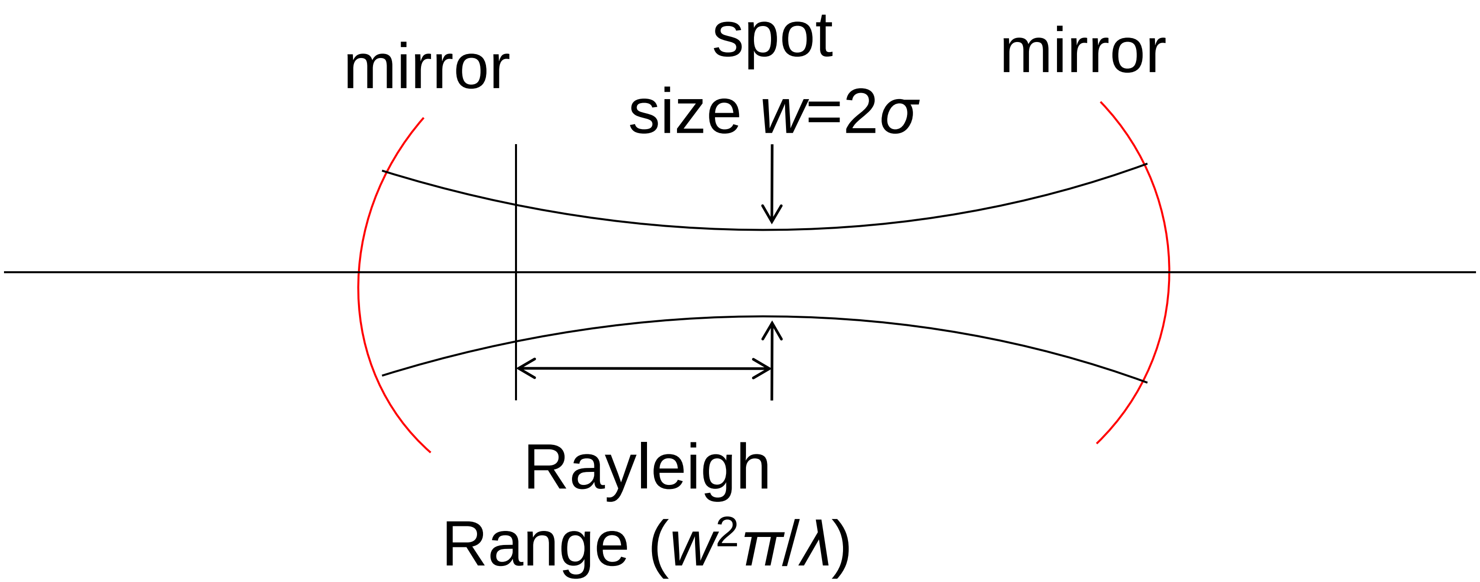

Quantity	Dimensions
Wavelength	200 nm-10 microns
Circulating Power	0.1-200 kW
Spot Size	50-500 microns
Rayleigh Range	40 cm-5 m

Self Excited

Location	Wavelength	Circulating Power	Spot Size	Rayleigh Range
Orsay	5 microns	100 W	mm	0.7 m
UVSOR	466 nm	20 W	250 microns	0.4 m
Duke Univ.	545 nm	1.6 kW	930 microns	5 m
Super-ACO	300 nm	190 W	440 microns	2 m
Jefferson Lab FEL	1 micron	100 kW	150 microns	1 m

Externally Excited

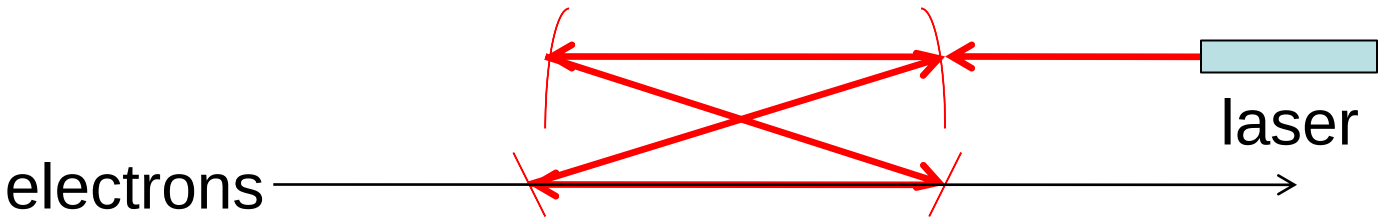

Location	Wavelength	Input Power	Circulating Power	Spot Size (rms)
Jefferson Lab Polarimeter	1064 nm	0.3 W	1.5 kW	120 microns
TERAS	1064 nm	0.5 W	7.5 W	900 microns
Lyncean	1064 nm	7 W	25 kW	60 microns
HERA Polarimeter	1064 nm	0.7 W	2 kW	200 microns
LAL	532 nm	1.0 W	10 kW	40 microns

Modern Ring Based Systems

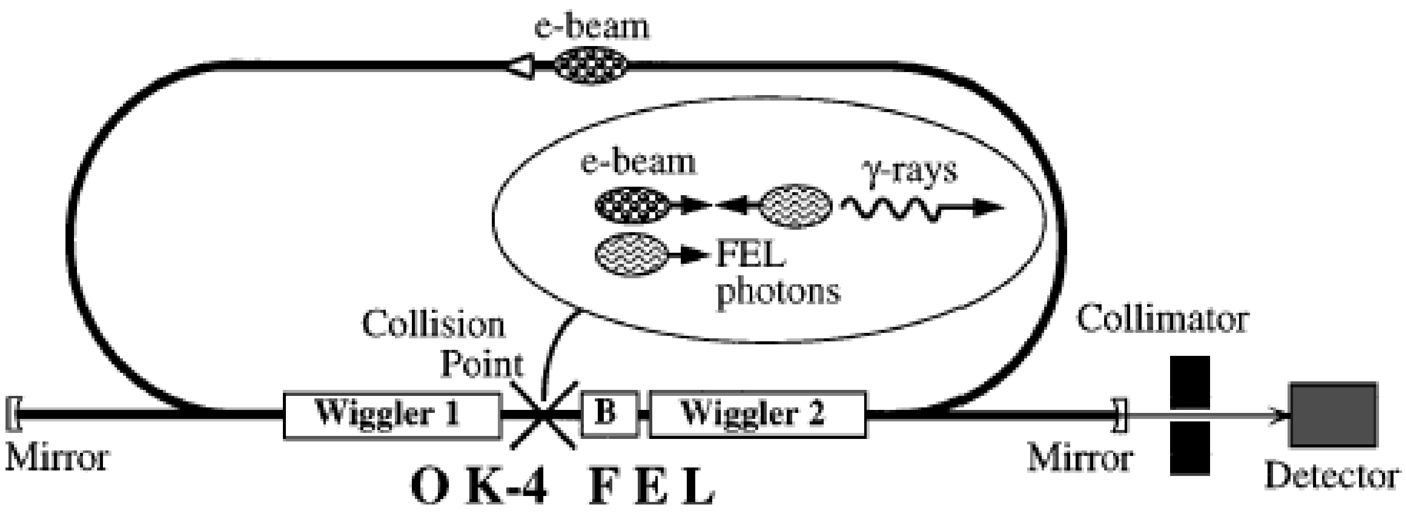

FIG. 1. Schematic of the OK-4/Duke storage ring FEL and γ-ray source. Two electron bunches spatially separated by one-half the circumference of the ring participate both in lasing and γ-ray production via Compton scattering of intracavity photons. A collimator installed downstream selects a narrow cone of quasimonoenergetic γ rays.

Litvinenko, *et al.*, *Phys. Rev. Lett.*, **78**, 4569 (1997)

Duke HIGS Facility

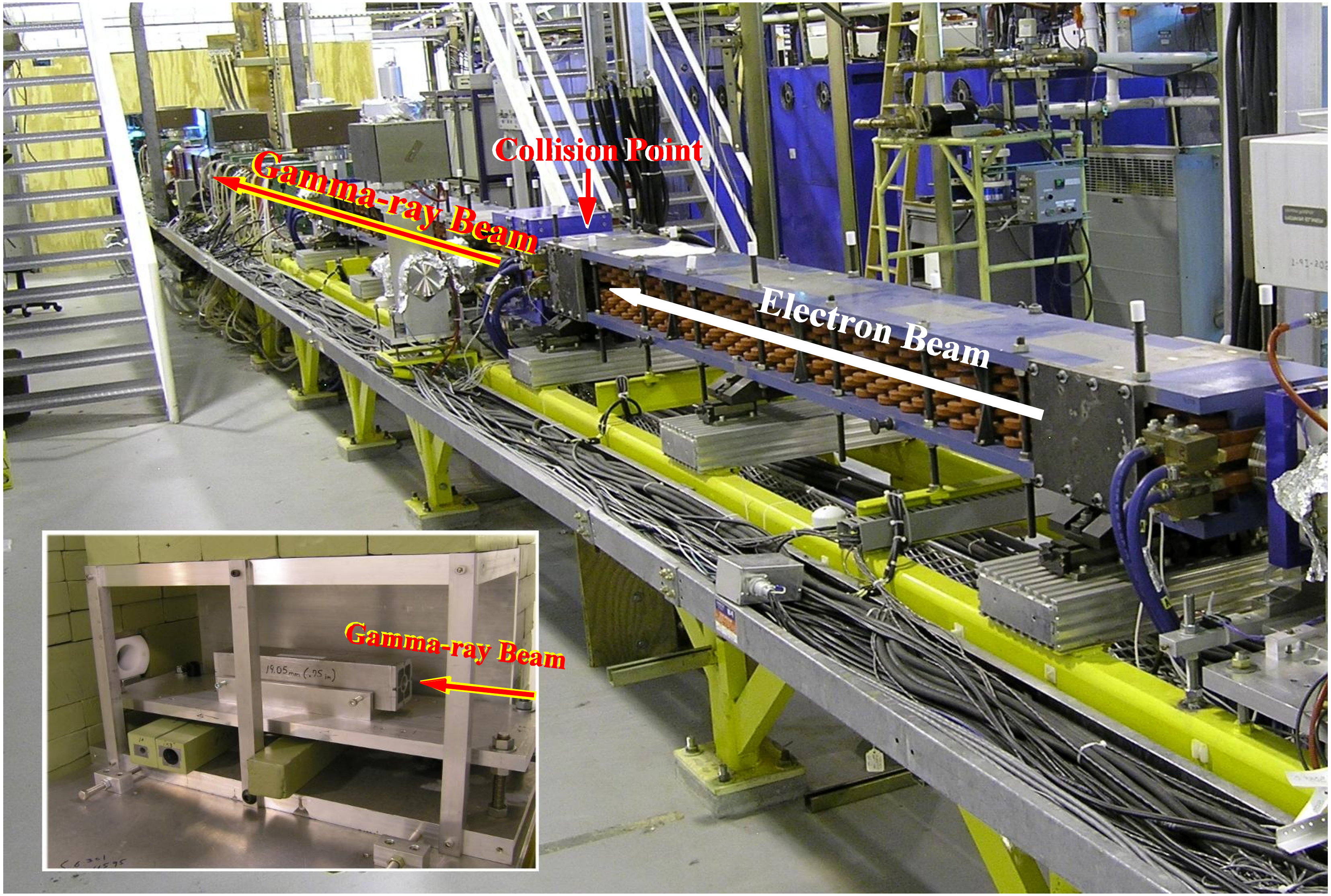

Some Modern Parameters

Parmeter	Value	Unit
Photon Energy	100	MeV
Production Rate	10^{10}	photons/sec@9 MeV
Laser Wavelength	545	nm
Circulating Power	1.6	kW
Polarization	100%	

Topoff allows larger circulating power now!

H. R. Weller, *et al.*, *Prog. Part. Nucl. Phys.*, **62**, 4569 (2009)

Lyncean Compact X-ray Source

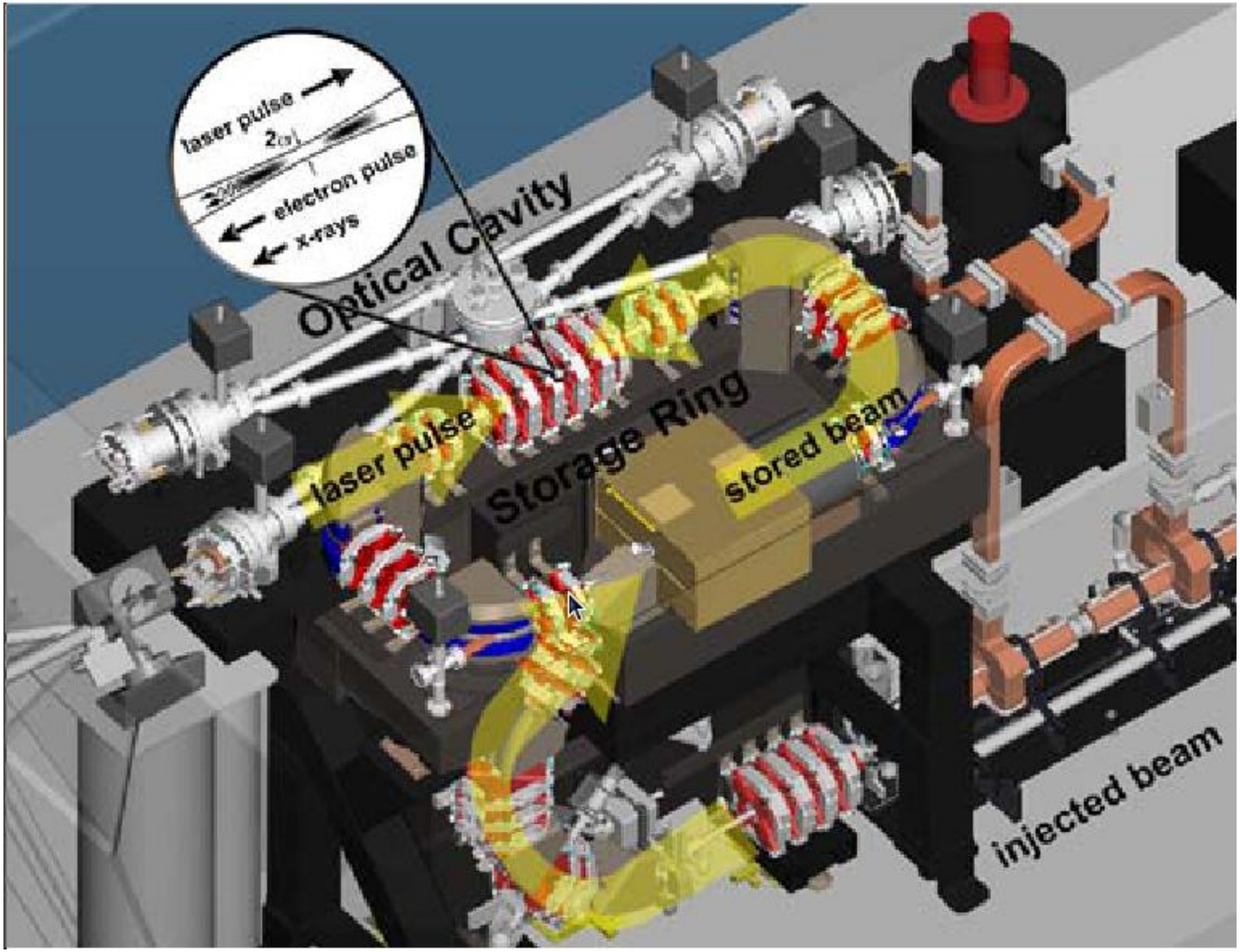

Lyncean Source Performance

Parmeter	Value	Unit
Photon Energy	10-20	keV
Production Rate	10^{11}	photons/sec
Laser Wavelength	1064	nm
Circulating Power	25	kW
Polarization	100%	
Ultimate Brilliance	$5 \ 10^{11}$	p/(sec mm^{2}mrad^{2}0.1%)

The Jefferson Lab IR FEL

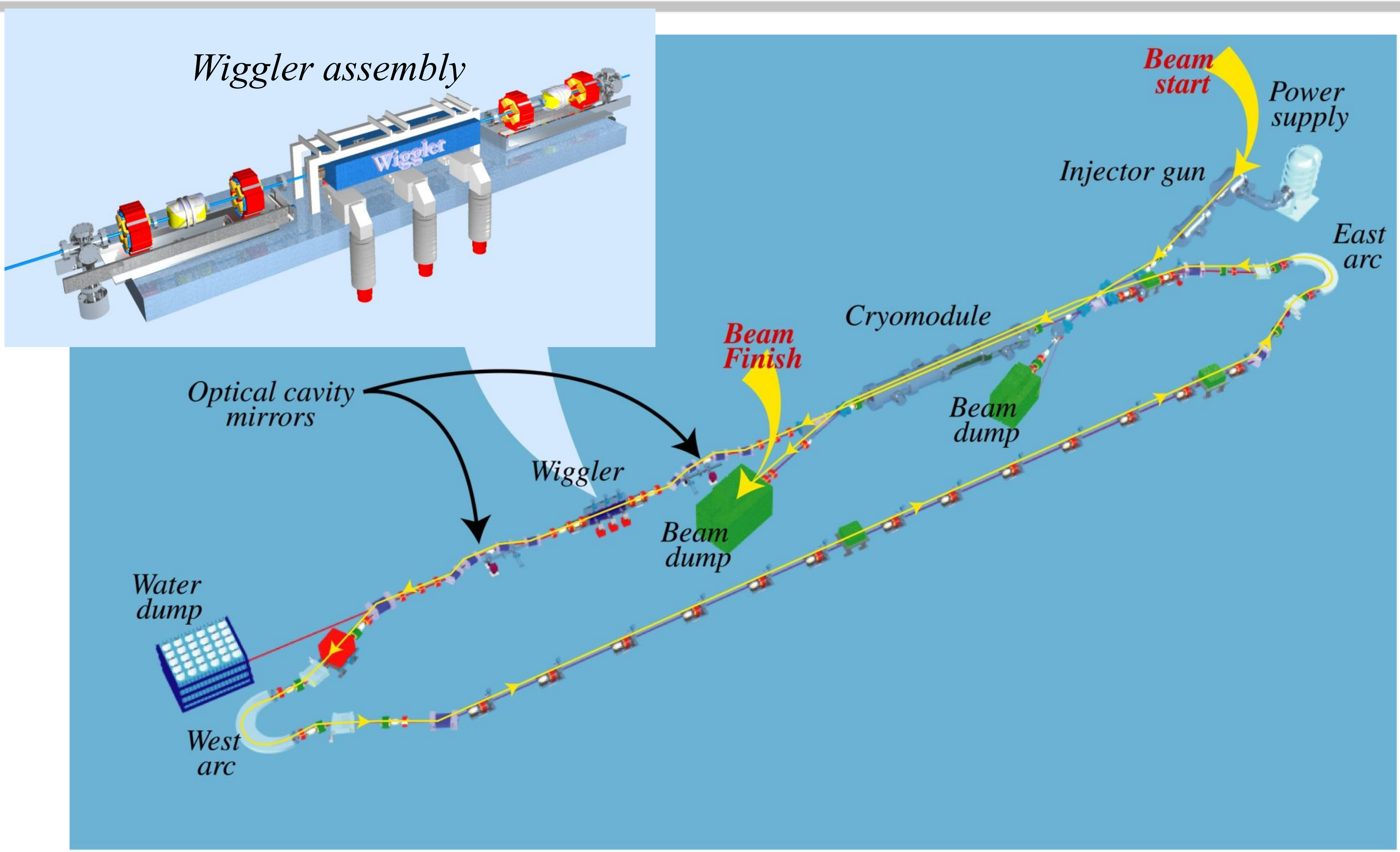

Neil, G. R., *et. al, Physical Review Letters,* **84,** 622 (2000)

FEL Accelerator Parameters

Parameter	Designed	Measured
Kinetic Energy	48 MeV	48.0 MeV
Average current	5 mA	4.8 mA
Bunch charge	60 pC	Up to 135 pC
Bunch length (rms)	<1 ps	0.4±0.1 ps
Peak current	22 A	Up to 60 A
Trans. Emittance (rms)	<8.7 mm-mr	7.5±1.5 mm-mr
Long. Emittance (rms)	33 keV-deg	26±7 keV-deg
Pulse repetition frequency (PRF)	18.7 MHz, x2	18.7 MHz, x0.25, x0.5, x2, and x4

Thomson Source Scattering Geometry

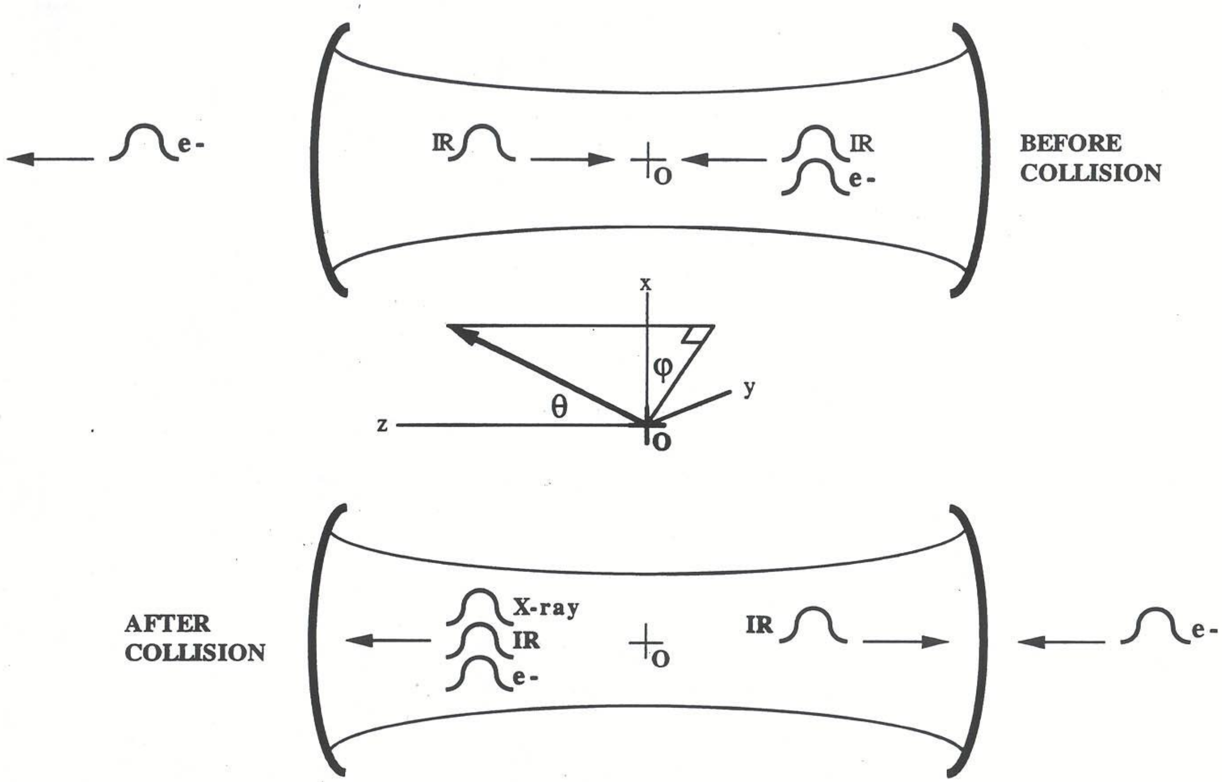

SCATTERING GEOMETRY

60 sec FEL Short-pulse X-ray Spectrum

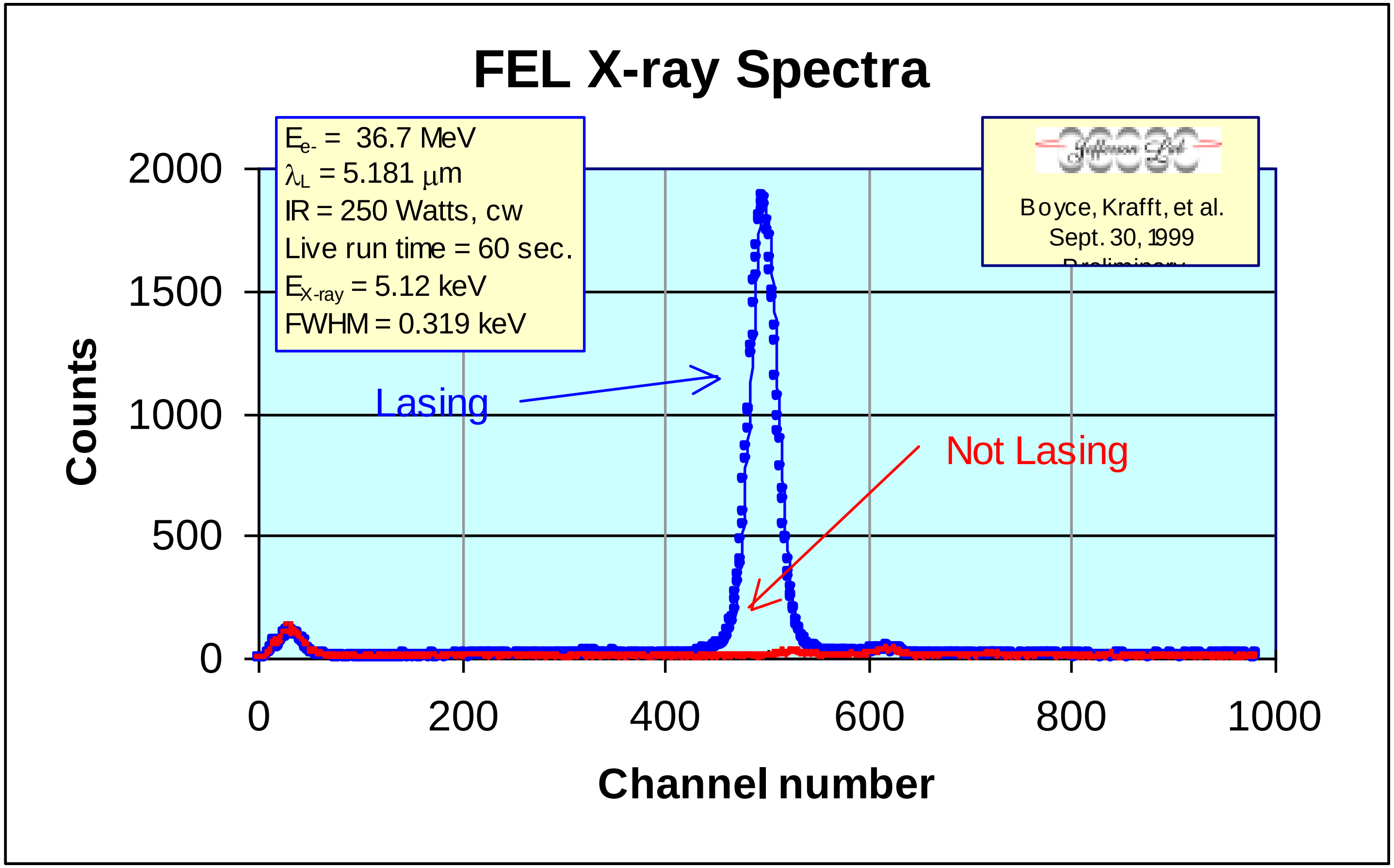

Boyce, *et al.*, 17^{th} Int. Conf. Appl. Accel., 325 (2002)

Linac-based Sources aka Blast Away

- Take the biggest laser you can get and focus to smallest spot you can
- Single shots at low repetition rate
- High peak brilliance (but not at FEL levels)

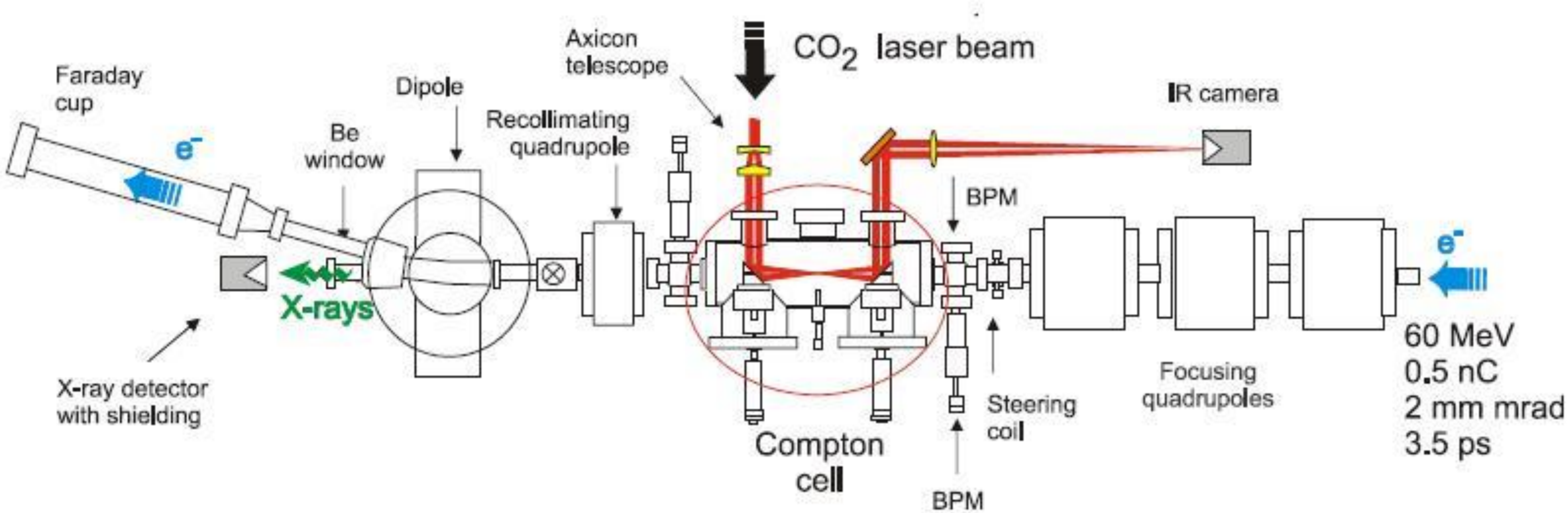

Pogorelsky, *et al., Phys. Rev. ST-AB*, **3**, 090702 (2000)
F. Albert, *et al., Phys. Rev. ST-AB*, **13**, 070704 (2010),
Daresbury ALICE Group

BNL Scattering Chamber

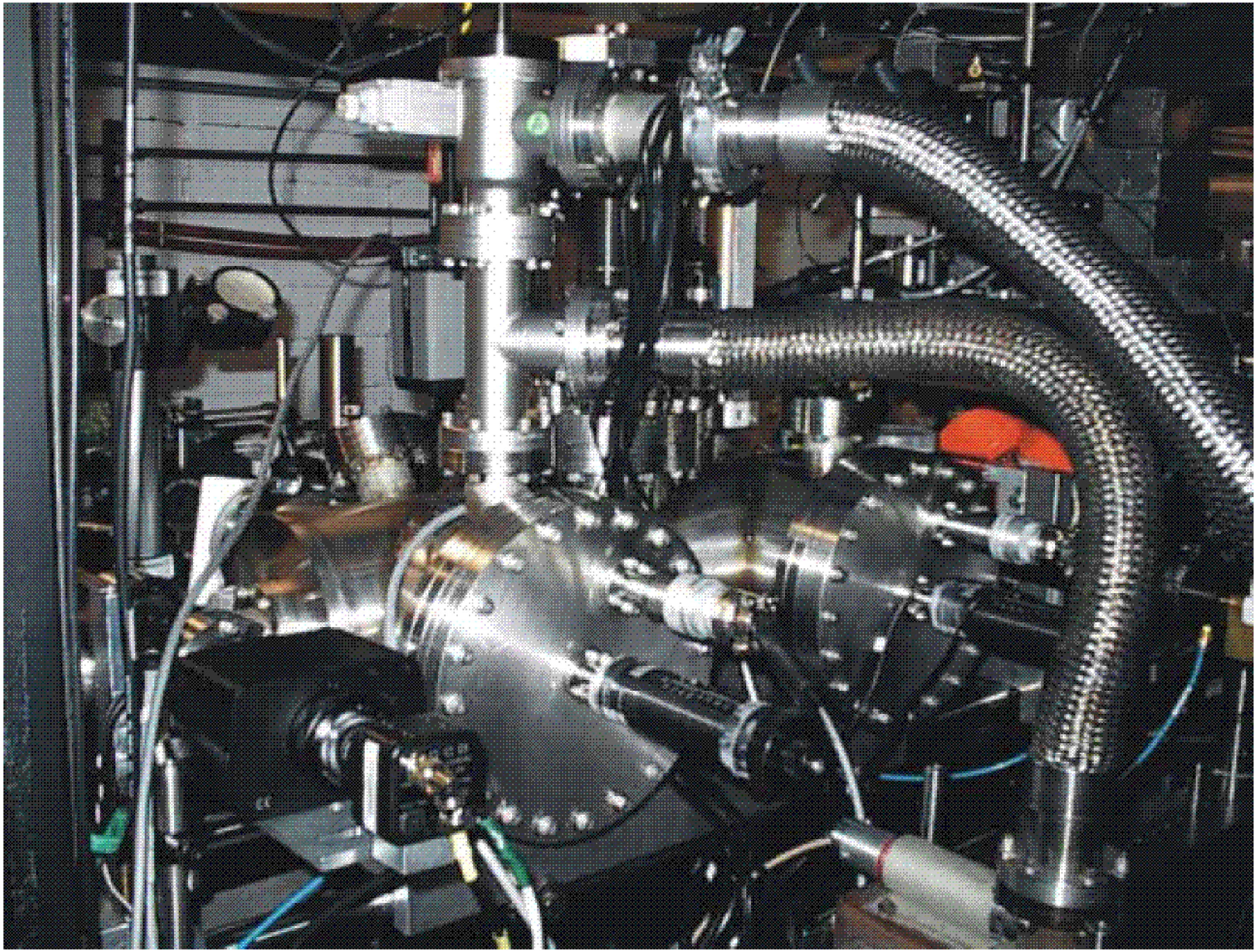

X-ray Experiment

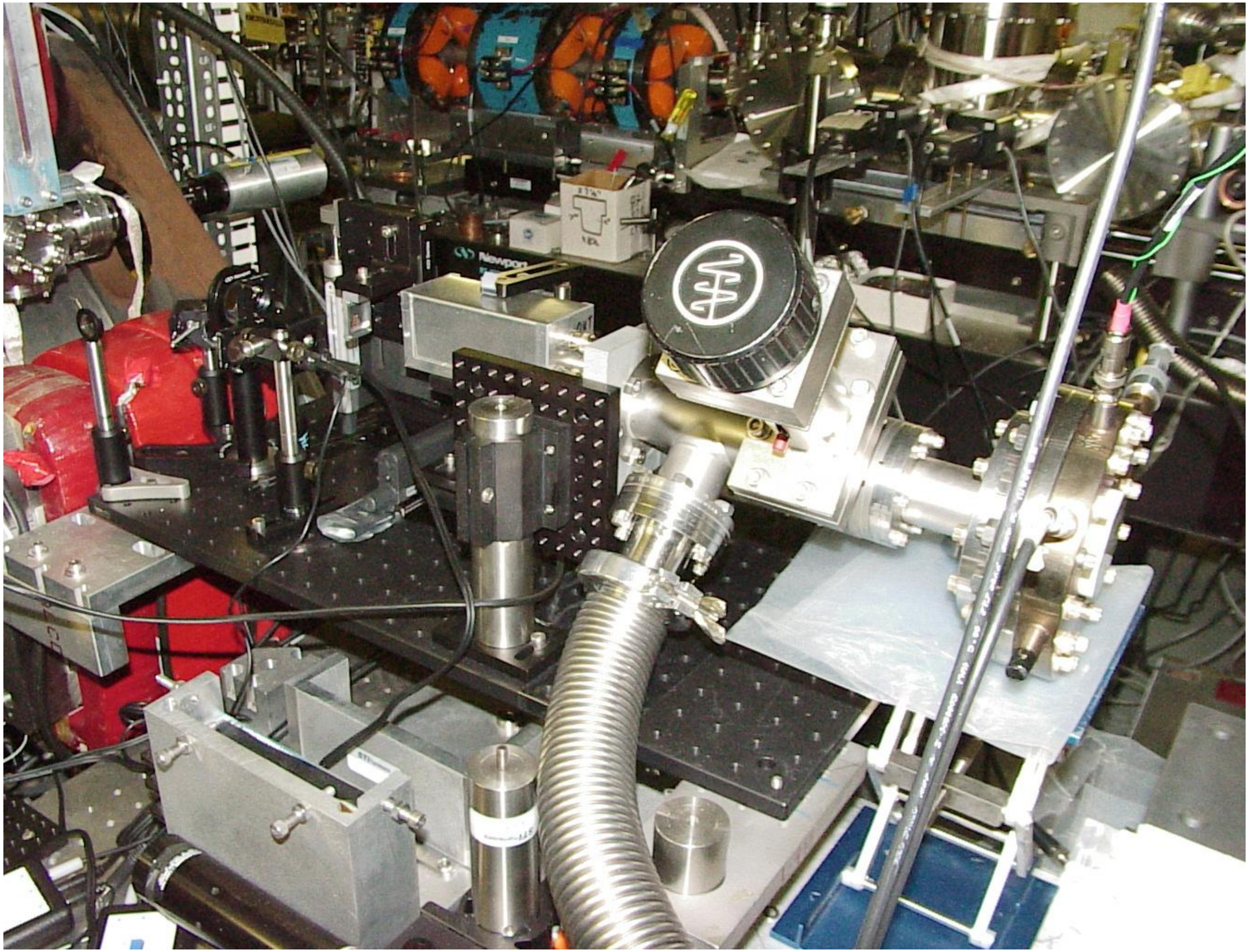

LLNL

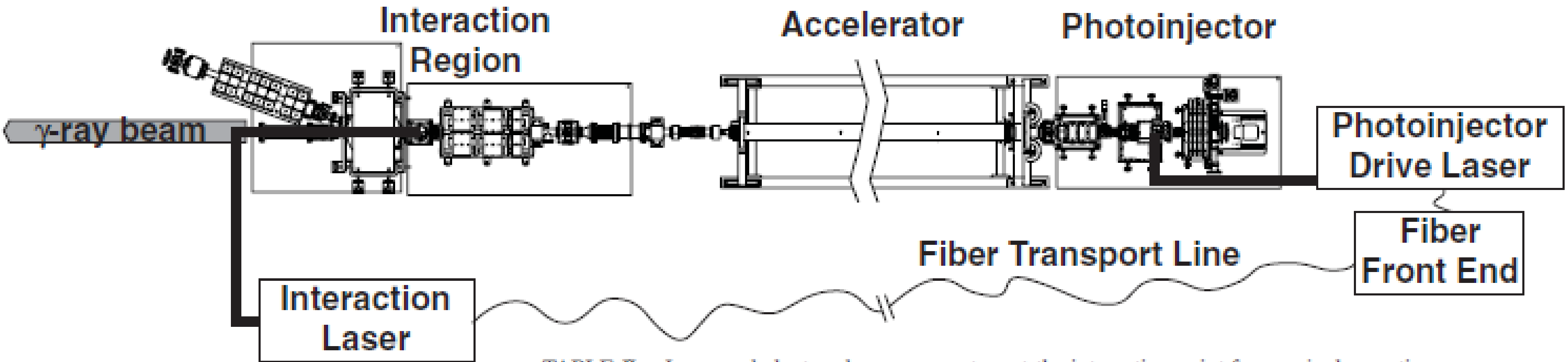

TABLE II. Laser and electron beam parameters at the interaction point for nominal operation.

Laser	
Repetition rate	10 Hz
Wavelength	532 nm
Bandwidth (FWHM)	0.1 nm
Total pulse energy[a]	150 mJ
Pulse length (FWHM)[b]	16 ps
rms spot size	$34 \times 38\ \mu m$
Electrons	
Repetition rate	10 Hz
Energy	116 MeV
rms energy spread	0.2%
Beam charge	800 pC
Bunch length (FWHM)	16 ps
rms spot size	$23 \times 42\ \mu m$
rms normalized emittance	4×8 mm mrad

[a]Energy in 100 μm aperture and 16 ps FWHM main pulse: 22 mJ. See text for details.
[b]Based on models of frequency conversion.

D. J.Gibson, *et al., Phys. Rev. ST-AB*, **13**, 070703 (2010)

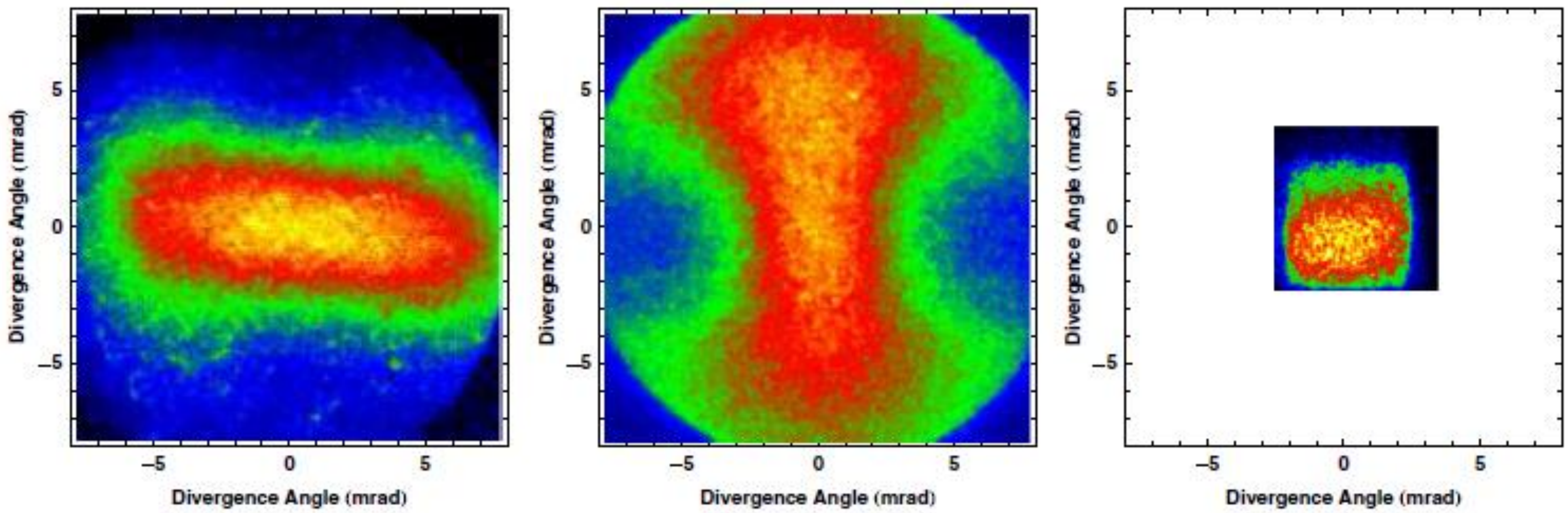

FIG. 10. (Color) γ-ray beam profiles from scintillator-coupled CCD cameras for the three laser frequencies. The beam energies are: left—295 keV (128.4 MeV + 1ω), center—466 keV (114 MeV + 2ω), and right—906 keV (130 MeV + 3ω).

TABLE III. Gamma source performance parameters.

Photons per interaction	1.6×10^5
Peak (on-axis) energy	478 keV
rms energy spread	12%
Repetition rate	10 Hz
Peak (on-axis) brightness	$1.5 \times 10^{15} \frac{\text{photons}}{\text{mm}^2\ \text{mrad}^2\ \text{s}\ 0.1\%\ \text{BW}}$
Inferred rms spot size	$\sim 36\ \mu\text{m}$
Beam divergence	10×6 mrad

High Power Optical Cavities

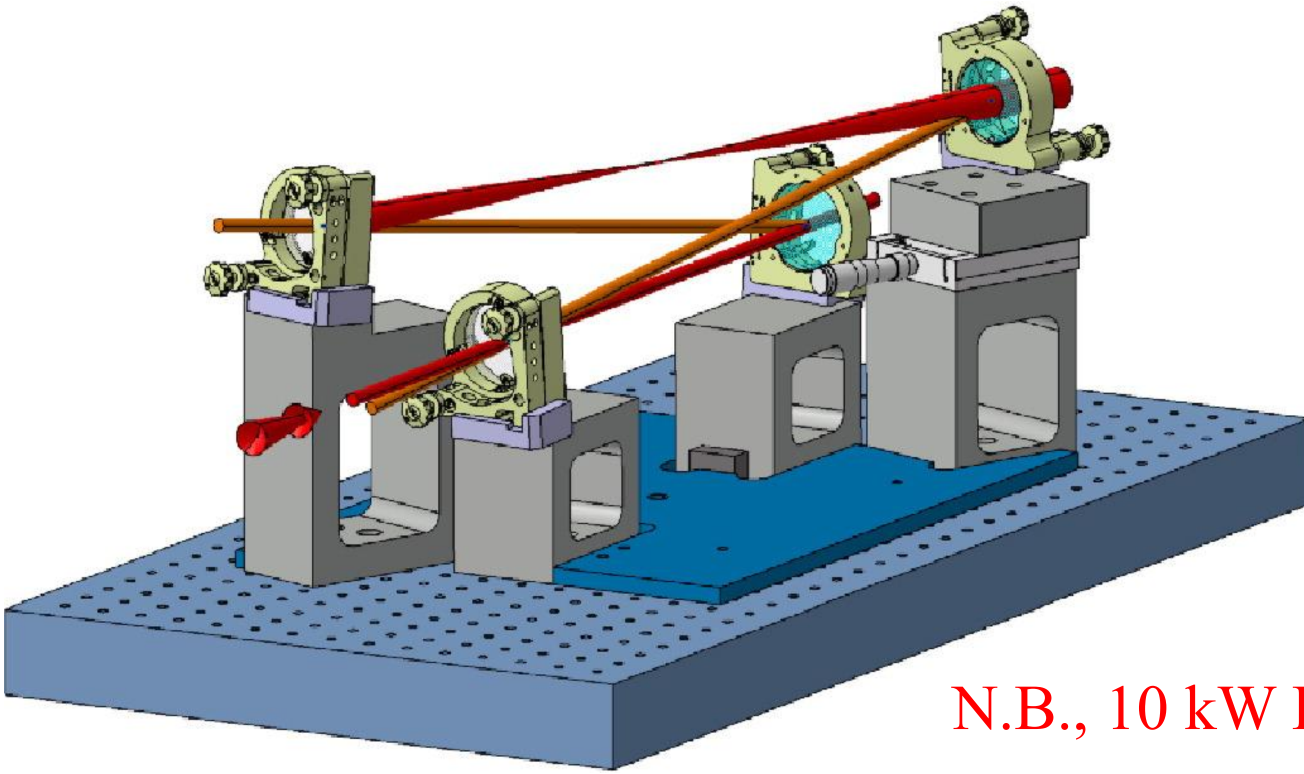

V. Brisson, *et al.*, *NIM A*, **608**, S75 (2009)

N.B., 10 kW FEL there, sans spot!

In this paper we described our first results on the locking of a Ti:sapph oscillator to a high finesse FPC. For the first time, to our knowledge, we demonstrate the possibility of stacking picosecond pulses inside an FPC at a very high repetition rate with a gain of the level of 10000. By studying the stability of four-mirrors resonators, we developed a new promising nonplanar geometry that we have just started to study experimentally. Finally, we mentioned that we shall next use the recent and powerful laser fiber amplification scheme to reach the megawatt average power inside FPC as required by the applications of the Compton X and gamma ray sources.

LAL/Thales THomX

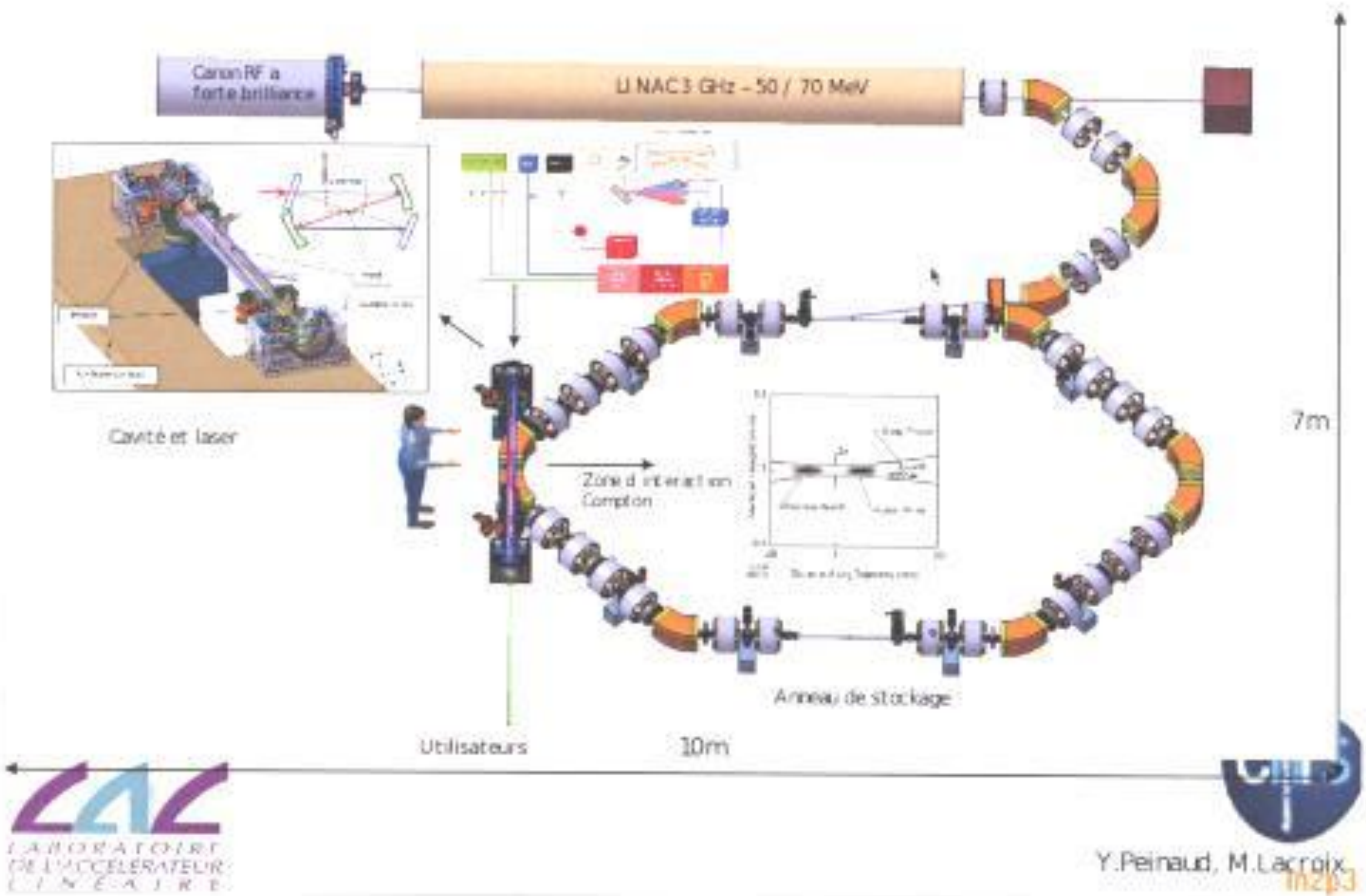

BES Workshop on Compact Light Sources (2010)

Hajima, et al.

Uranium Detection

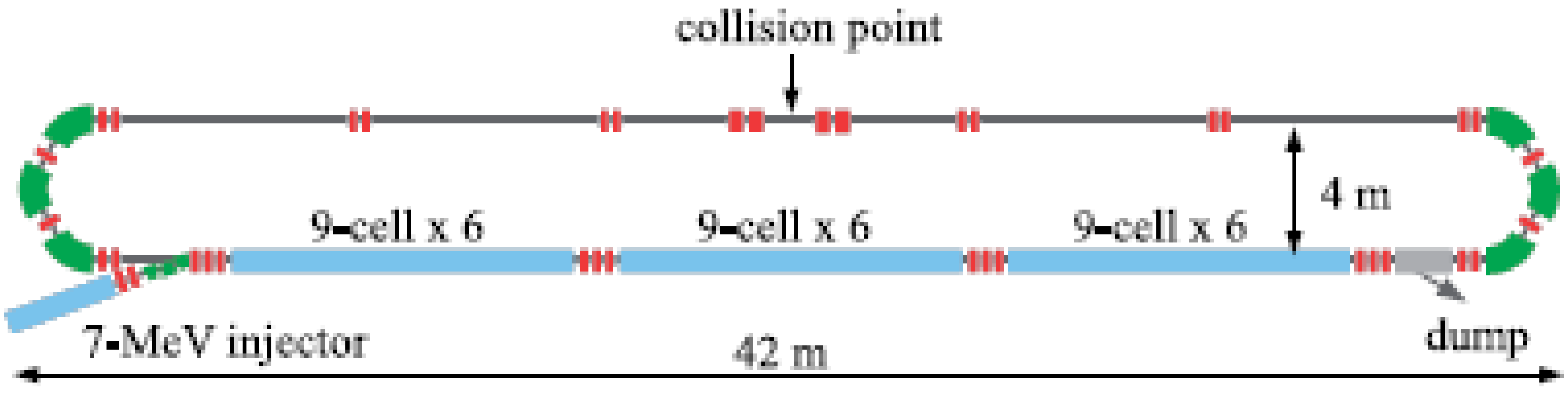

Fig. 3. Layout of the 350-MeV ERL designed for a high-flux γ-ray source. An electron beam generated by the 7-MeV injector is accelerated up to 350 MeV by the main linac and transported to the recirculation loop. The collision point for LCS γ-ray generation is located in the middle of the straight section.

Hajima, *et al.*, *NIM A*, **608**, S57 (2009)

TRIUMF Moly Source?

Table 1
Design parameters of a high-flux γ-ray facility.

Electron beam	
Maximum energy	350 MeV
Current	13 mA
Bunch charge	100 pC
Normalized emittance (*x*/*y*)	2.2/1.0 mm–mrad
Laser and laser supercavity	
Laser	1.8 μJ, 1064 nm
Repetition rate	130 MHz
Supercavity gain	3000
γ-ray	
Total flux	1.0×10^{13} ph/s

In the design, we consider a laser supercavity that stores an intracavity laser power of 700 kW (1.8 μJ, 130 MHz, gain of 3000, Rayleigh length of 1.1 cm). The γ-ray flux in the above-mentioned

MIT CUBiX

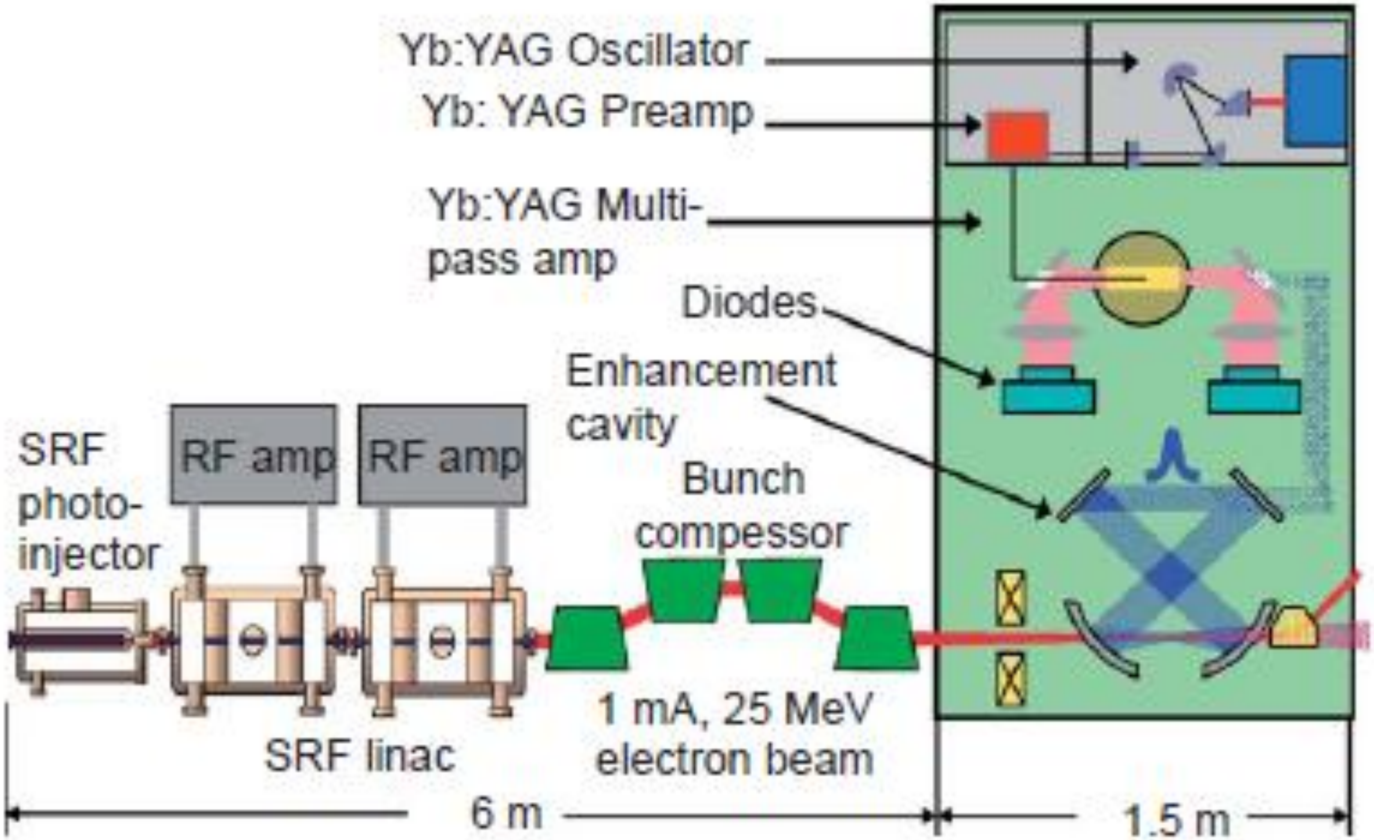

Fig. 2. Major technical components including cryocooled high-power laser and SRF linac.

Graves, *et al.*, *NIM A*, **608**, S103 (2009)

Table 1
X-ray parameters.

Parameter	Single shot	High flux
Tunable photon energy (keV)	3–30	
Pulse length (ps)	2	0.1
Flux per shot (photons)	1×10^{10}	3×10^{6}
Repetition rate (Hz)	10	10^{8}
Average flux (photons/s)	1×10^{11}	3×10^{14}
On-axis bandwidth (%)	2	1
RMS divergence (mrad)	5	1
Source RMS size (mm)	0.006	0.002
Peak brilliance (photons/(s mm^2 mrad^2 0.1%bw))	6×10^{22}	6×10^{19}
Average brilliance (photons/(s mm^2 mrad^2 0.1%bw))	6×10^{11}	2×10^{15}

numerical simulation results assuming parameters of $E = 25\,\text{MeV}$, $\varepsilon_{nx} = 0.1\ \mu\text{m}$, $x_e = 2\ \mu\text{m}$, $\Delta t_L = 0.3\ \text{ps}$, $\lambda = 1\ \mu\text{m}$, $Q_e = 10\,\text{pc}$, and $W_\gamma = 10$ mJ. Note that no nonlinear effects were included in this

Quarter Wave SRF Injector

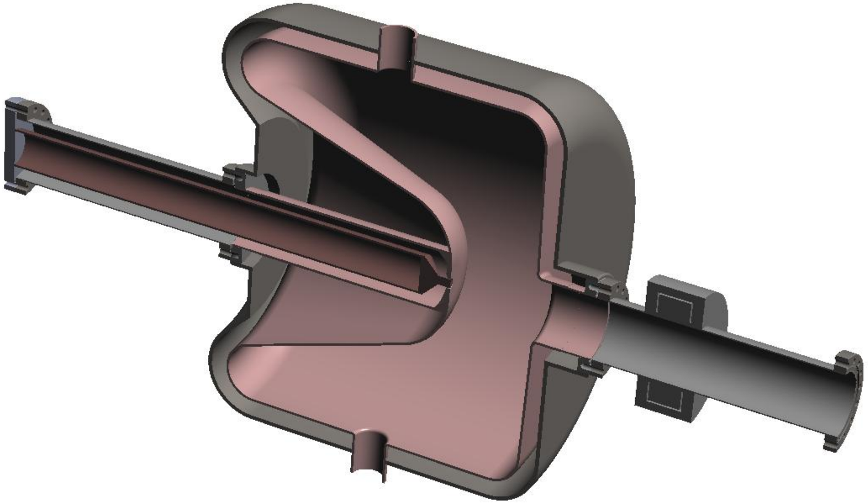

SRF Injector Parameters	
Energy gain [MeV]	4
RF frequency [MHz]	176
Average current [mA]	1
Operating temperature [K]	4.2
RF power [kW]	5
Peak wall E-field [MV/m]	55
Peak wall B-field [mT]	105
Accelerating E-field [MV/m]	32
Cathode E-field [MV/m]	45

Developed in collaborations with Niowave Inc, UW-Madison, Naval Postgraduate School

G. A. Krafft, CUBiX NSF Review (2010)

4K SRF CW Linac

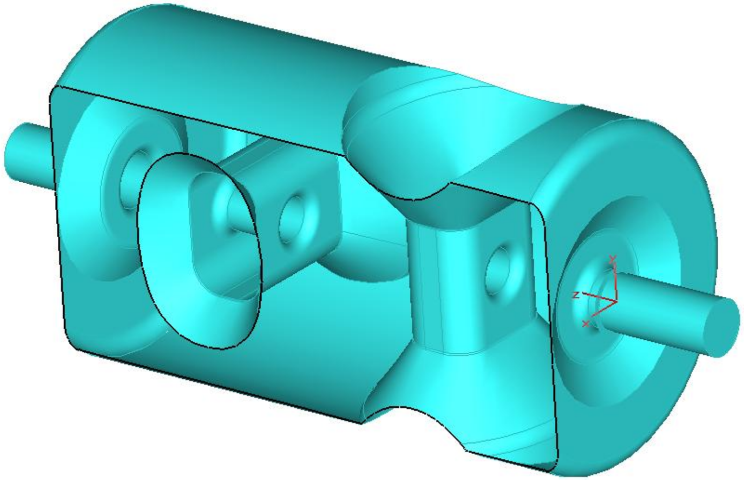

SRF Linac Parameters	
Energy gain [MeV]	25
RF frequency [MHz]	352
Average current [mA]	1
Operating temperature [K]	4.2
RF power [kW]	30

Jean Delayen developing cavities at newly formed Center for Accelerator Science at Old Dominion University (Chris Hopper of ODU/CASA) has a velocity-of-light design

4 K SRF Technology: Spoke cavities

Lower RF frequency => 4K operation

More compact for given frequency

Good mechanical rigidity

Moderate gradient (10 - 12 MV/m CW)

Longitudinal Compression Ideas

- Transverse displacement

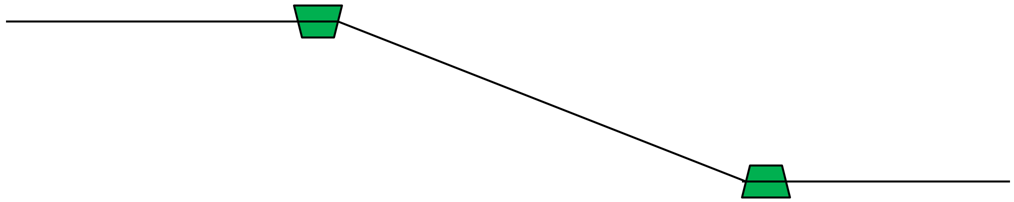

- Modified chicane

- Modified "π" bend

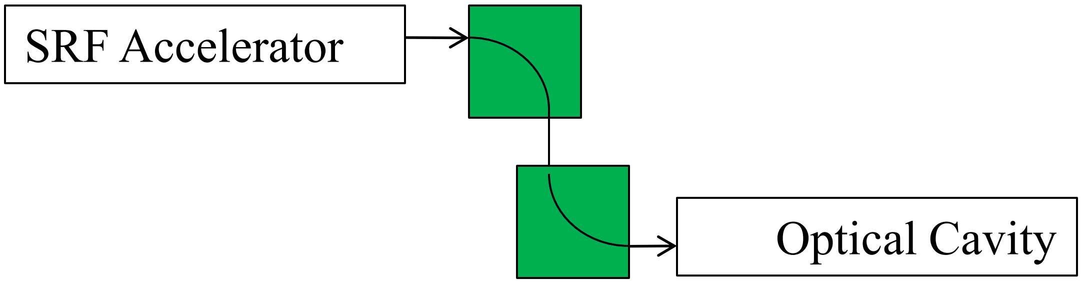

SPARC

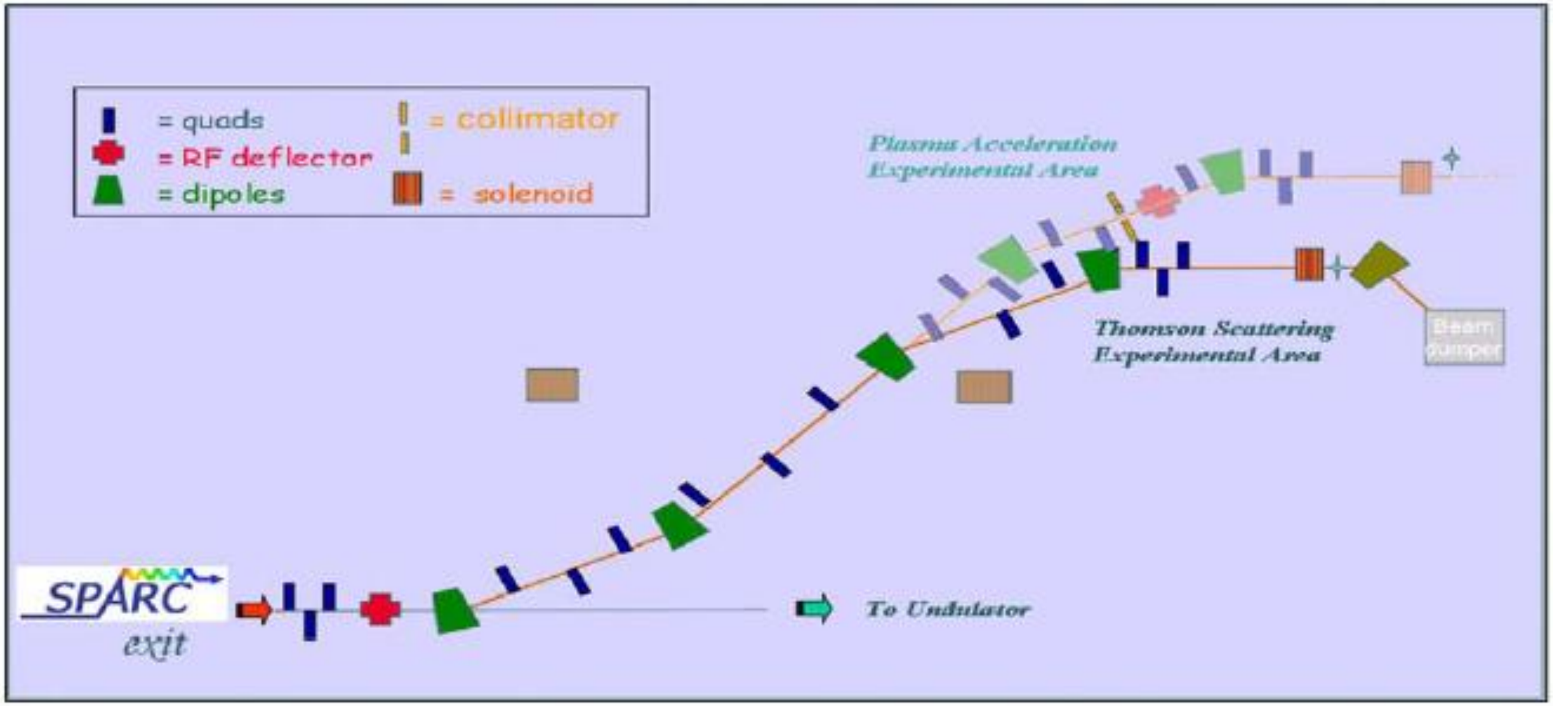

Fig. 1. Lay-out of the dog-leg like electron beam line for the TS experimental area.

A. Bacci, *et al.*, *NIM A*, **608**, S90 (2009)

Table 1
Electron beam at the interaction point.

Parameter	Value
Bunch charge (nC)	1–2
Energy (MeV)	28–150
Length (ps)	15–20
$\varepsilon_{n\_x,y}$ (mm-mrad)	1–5
Energy spread (%)	0.05*–0.2
Spot size at interaction point rms (μm)	5–10

Conclusions

- Compton sources of high energy photons have existed for about thirty years
- The have followed the usual progression: [1] borrow an existing machine (1^{st} generation), and [2] make it better by technological innovation (2^{nd} generation?)
- We are perhaps approaching 3^{rd} generation devices, i.e., accelerators specifically designed for Compton/Thomson sources.
- Expect "convergence" with high energy collider design ideas
- Lots of ideas, but still looking for the "killer ap".

Conclusions

- A “new” calculation scheme for high intensity pulsed laser Thomson Scattering has been developed. This same scheme can be applied to calculate spectral properties of “short”, high-*K* wigglers.
- Due to ponderomotive broadening, it is simply wrong to use single-frequency estimates of flux and brilliance in situations where the square of the field strength parameter becomes comparable to or exceeds the (1/*N*) spectral width of the induced electron wiggle
- The new theory is especially useful when considering Thomson scattering of Table Top TeraWatt lasers, which have exceedingly high field and short pulses. Any calculation that does not include ponderomotive broadening is incorrect.

Bend

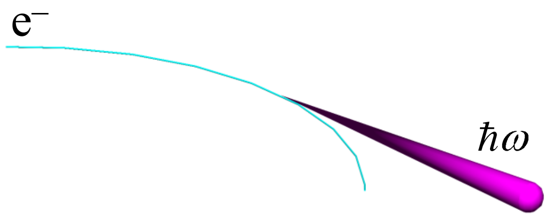

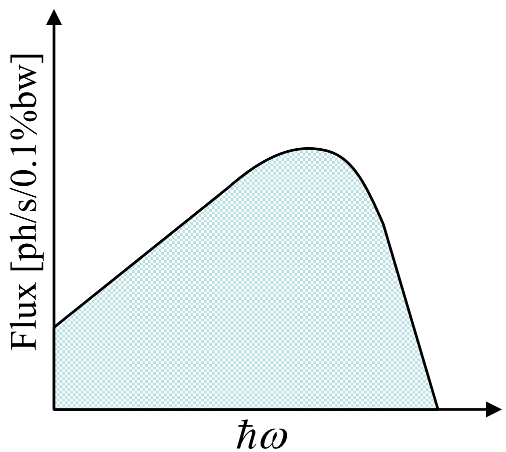

white source

Undulator

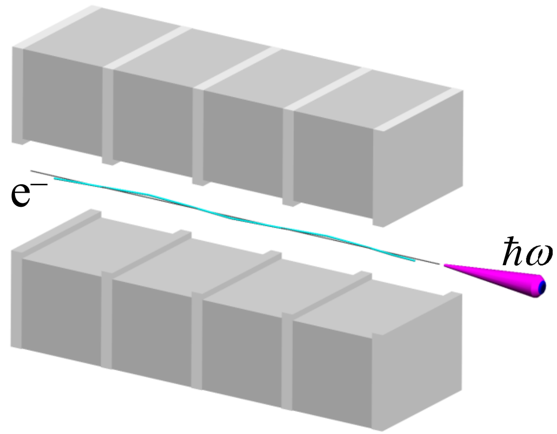

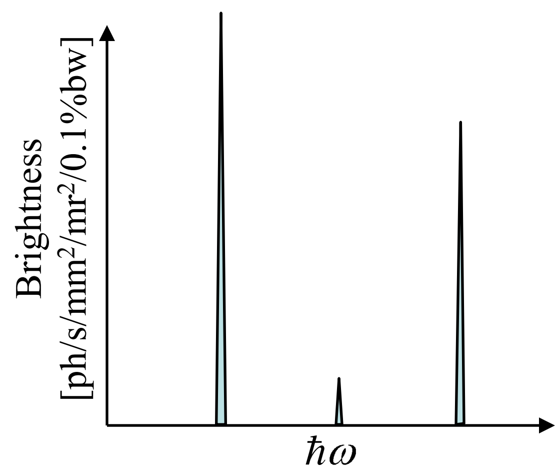

partially coherent source

Wiggler

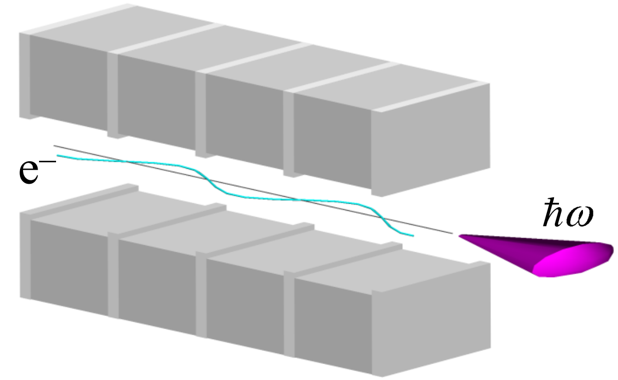

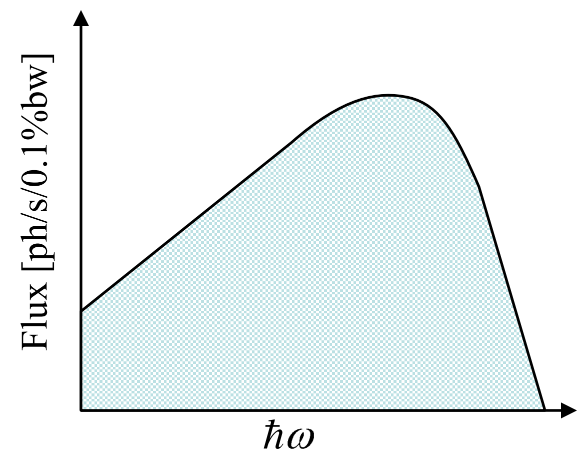

powerful white source